H2AEOLUS

Deliverable D6.4

Control system for fuel-production use case

Public

M. B. Abdelghany, M. F. Shehzad, V. Mariani, D. Liuzza, L. Glielmo (UniSannio)

Quality Assurance: F. Zenith (SINTEF)

Project acronym:	Haeolus
Project title:	Hydrogen-Aeolic Energy with Optimised eLectrolysers Upstream of Substation
Project number:	779469
Call:	H2020-JTI-FCH-2017-1
Topic:	FCH-02-4-2017
Document date:	February 5, 2021
Due date:	December 31, 2020
Keywords:	Energy storage systems, hydrogen conversion, power to gas, energy management, model predictive control, mixed logical dynamical

Abstract: The current deliverable explains the formulation of a Model Predictive Control (MPC) policy for a wind-hydrogen plant in fuel-production use cases within the EU-FCH 2 JU (European Union Fuel Cells and Hydrogen 2 Joint Undertaking) funded project HAEOLUS.
In the fuel-production control algorithm, hydrogen production objectives are two-fold: to deliver hydrogen as a fuel to (road) vehicles and to provide a demand and generation management solution for energy supply modulation. Given the name of the control algorithm, of course, the priority comes first with the first objective, and then any excess of stored hydrogen will be re-electrified through fuel cell in meeting electrical references.
This goal is achieved through a multi-level MPC that takes into account external hydrogen consumer requests, optimal load demand tracking, and electricity market participation. In order to achieve a feasible electrolyzer and fuel cell operation policies, the devices are modeled by means of the Mixed Logical Dynamical (MLD) framework in both continuous/discrete dynamics and switching between different operating conditions.

Revision History

Date	Description	Author (organisation)
2020/May/10	First draft	Muhammad Bakr Abdelghany (UniSannio)
2020/May/15	Add Abstract, Introduction	Muhammad Bakr Abdelghany (UniSannio)
2020/May/25	Add System modeling	Muhammad Bakr Abdelghany (UniSannio)
2019/June/12	Controller Design	Muhammad Bakr Abdelghany (UniSannio)
2019/June/22	Controller Design	Muhammad Bakr Abdelghany (UniSannio)
2019/July/20	Updated Controller	Muhammad Bakr Abdelghany (UniSannio)
2020/August/29	Updated Abstract	Muhammad Bakr Abdelghany (UniSannio)
2020/September/4	Updated Introduction	Muhammad Bakr Abdelghany (UniSannio)
2020/September/10	Revision	Valerio Mariani (UniSannio)
2020/September/12	Updated Introduction	Muhammad Bakr Abdelghany (UniSannio)
2020/September/14	Updated Modelling	Muhammad Bakr Abdelghany (UniSannio)
2020/September/16	Updated Controller	Muhammad Bakr Abdelghany (UniSannio)
2020/September/23	Revision	Valerio Mariani (UniSannio)
2020/September/24	Updated Modelling	Muhammad Bakr Abdelghany (UniSannio)
2020/September/28	Updated Controller	Muhammad Bakr Abdelghany (UniSannio)
2020/October/07	Review text for issues and inconsistencies fixing	Valerio Mariani (UniSannio)
2020/October/27	Revisions addressed	Muhammad Bakr Abdelghany (UniSannio)
2020/November/07	Review text for issues and inconsistencies fixing	Valerio Mariani (UniSannio)
2020/November/27	Revisions addressed	Muhammad Bakr Abdelghany (UniSannio)
2020/December/02	Review text for issues and inconsistencies fixing	Valerio Mariani (UniSannio)
2020/December/4	Revisions addressed	Muhammad Bakr Abdelghany (UniSannio)
2021/January/10	Added simulation section	Muhammad Bakr Abdelghany (UniSannio)

This project has received funding from the Fuel Cells and Hydrogen 2 Joint Undertaking under the European Union's Horizon 2020 research and innovation programme under grant agreement Nº 779469.

Any contents herein reflect solely the authors' view. The FCH 2 JU and the European Commission are not responsible for any use that may be made of the information herein contained.

Table of Contents

1 Introduction

In the previous deliverables (D6.1 [1], D6.2 [2], and D6.3 [3]), the dynamic plant models for the wind-hydrogen system, the energy storage and the mini-grid use cases for the HAEOLUS plant have been delivered. The corresponding proposed controllers were able to smooth out short-term fluctuations in wind power and to solve two different time-scales of the electricity market: the intraday market (day ahead) with a long term horizon and the real-time market with a short term horizon.

In this deliverable, the alternative technologies to power road vehicles considered by the International Energy Agency (IEA) as being capable of delivering a sustainable road transport system with near-zero emissions are addressed. In particular, hydrogen is considered as fuel for road transport. The design criterion is that the proposed hydrogen-based wind farm attempts to satisfy hydrogen demand from external agents, i.e., Fuel Cell Electric Vehicles (FCEV), and for the participation to the electricity market by exchanging power though grid utilization further enforcing the fulfillment of the physical and the system's dynamics constraints.

The considered scenario corresponds to the definition in the IEA-HIA Task 24 final report for wind farm use cases under the category of fuel production where it is reported that "*The main purpose of facilities under this category is supplying hydrogen fuel to (road) vehicles. The simplest mode [...] would be to produce and store hydrogen continuously [...] to satisfy the average fuel demand. However, this plays no role in the management of wind power [...]. In terms of energy security and climate change, significant benefits are gained in operating electrolysers in a more responsive, and grid-balancing mode. In this case, the electrolysers [...] respond to the supply and demand balance of the grid. This is rewarded through flexible tariffs and price signals on the spot market [...]*" [4].

Therefore, we develop a hierarchical control architecture and control algorithms in order to fulfill hydrogen demands for commercial vehicles with higher priority. In addition to the hydrogen demand fulfillment, any excess of renewable energy generation will be sold to the electricity market and used for supplying a local load with tunable priorities.

The fuel production use case is developed, solved, and experimentally validated under a complete 24-h test with sample times of T_s = 1 hour and T_s = 1 min according to the considered control layer.

2 Nomenclature

The parameters, the forecasts and the decision variables used in the proposed formulation are described in Table 1, Table 2 and Table 3, respectively.

2.1 Preliminaries and Notation

Throughout the document, we will use and agree on the following notation and facts unless otherwise specified. Boolean signals, used to represent discrete dynamics, are signals whose values are restricted to false (denoted by 0) and true (denoted by 1). Scalars are denoted by lowercase, non-bold letters; column vectors are indicated by lowercase, bold letters; matrices are denoted by uppercase, non-bold letters. We define the set $I = \{e, f\}$,

Table 1: Parameters

Parameters	Description
H^{max}	Maximum level of the hydrogen storage unit [kg]
H^{min}	Minimum level of the hydrogen storage unit [kg]
P_e^{max}	Maximum power level of the electrolyzer [kW]
P_e^{min}	Minimum power level of the electrolyzer [kW]
P_e^{CLD}	Power required by the electrolyzer for cold starts [kW]
P_e^{STB}	Power required by the electrolyzer in standby [kW]
P_e^{WRM}	Power required by the electrolyzer for warm starts [kW]
P_f^{max}	Maximum power level of the fuel cell [kW]
P_f^{min}	Minimum power level of the fuel cell [kW]
P_f^{CLD}	Power required by the fuel cell for cold starts [kW]
P_f^{STB}	Power required by the fuel cell in standby [kW]
P_f^{WRM}	Power required by the fuel cell for warm starts [kW]
η_e	Efficiency for the electrolyzer
η_f	Efficiency for the fuel cell
Cycles	Number of life cycles
NH_e	Number of life hours of the electrolyzer [h]
NH_f	Number of life hours of the fuel cell [h]
HY_f	Number of per year life hours of the fuel cell [h]
HY_e	Number of per year life hours of the electrolyzer [h]
$S_{rep,e}$	Electrolyzer stack replacement cost [€/kW]
$S_{rep,f}$	Fuel cell stack replacement cost [€/kW]
T_s	Sampling period [h]
T	Simulation horizon [h]
Γ^{sale}	Intraday energy price [€/kW h]

Table 2: Forecasted powers.

Forecasts	Description
P_w	Wind power production [kW]
H_{ref}	Hydrogen reference demand [kW]

Table 3: Real and logical variables.

Variables	Description
$\sigma^{\beta}_{\alpha,e}$	State transitions of the electrolyzer
$\sigma^{\beta}_{\alpha,f}$	State transitions of the fuel cell
$z_i^{\geq \gamma}$	Electric power formulated as mixed logical dynamical (MLD) variable
$z_i^{\leq \bar{\gamma}}$	Electric power formulated as mixed logical dynamical (MLD) variable
δ_e^{ON}	Logical variable corresponding to on state of the electrolyzer
δ_e^{OFF}	Logical variable corresponding to off state of the electrolyzer
δ_e^{STB}	Logical variable corresponding to standby state of the electrolyzer
δ_e^{CLD}	Logical variable corresponding to cold state of the electrolyzer
δ_e^{WRM}	Logical variable corresponding to warm up state of the electrolyzer
δ_f^{ON}	Logical variable corresponding to on state of the fuel cell
δ_f^{OFF}	Logical variable corresponding to off state of the fuel cell
δ_f^{STB}	Logical variable corresponding to standby state of the fuel cell
δ_f^{CLD}	Logical variable corresponding to cold state of the fuel cell
δ_f^{WRM}	Logical variable corresponding to warm up state of the fuel cell
P_e	Electrical power of the electrolyzer [kW]
P_f	Electrical power of the fuel cell [kW]
P_{avl}	Available power delivered to the grid [kW]
H	Stored level of the hydrogen [kg]
P_{grid}	Grid power [kW]

where "e" stands for "electrolyzer" and "f" stands for "fuel cell", and whenever needed we will index the relevant equations with $i \in I$. We define the sets $A^{\text{HL}} = \{\text{OFF}, \text{STB}, \text{ON}\}$ and $A^{\text{LL}} = \{\text{OFF}, \text{CLD}, \text{STB}, \text{WRM}, \text{ON}\}$ of the possible logic states for the electrolyzer's and the fuel cell's corresponding high-level and low-level automata, respectively, and the two indexes α, β with $\alpha \neq \beta$ which we assume will always take value in them. It will be clear from the context whether they take value in A^{HL} of in A^{LL}. Then, we define the sets $J^{\text{HL}} = \{0, P_i^{\text{STB}}, P_i^{\text{min}}\}$, $\bar{J}^{\text{HL}} = \{0, P_i^{\text{STB}}, P_i^{\text{max}}\}$, $J^{\text{LL}} = \{0, P_i^{\text{CLD}}, P_i^{\text{STB}}, P_i^{\text{WRM}}, P_i^{\text{min}}\}$, $\bar{J}^{\text{LL}} = \{0, P_i^{\text{CLD}}, P_i^{\text{STB}}, P_i^{\text{WRM}}, P_i^{\text{max}}\}$ and $G = \{\text{sale}, \text{pur}\}$. We define further sets $P^{\text{HL}} = \{(\gamma, \bar{\gamma}) \mid \gamma = \bar{\gamma} \vee (\gamma = P_i^{\text{min}} \wedge \bar{\gamma} = P_i^{\text{max}}),\ \gamma \in J^{\text{HL}},\ \bar{\gamma} \in \bar{J}^{\text{HL}}\}$ and $P^{\text{LL}} = \{(\gamma, \bar{\gamma}) \mid \gamma = \bar{\gamma} \vee (\gamma = P_i^{\text{min}} \wedge \bar{\gamma} = P_i^{\text{max}}),\ \gamma \in J^{\text{LL}},\ \bar{\gamma} \in \bar{J}^{\text{LL}}\}$. For reader's convenience the sets so far defined are reported in Table. 4.

Table 4: List of sets used in this report.

Set
I={e, f}
A^{LL}={OFF, CLD, STB, WRM, ON}
A^{HL}={OFF, STB, ON}
$J^{\text{LL}} = \{0, P_i^{\text{CLD}}, P_i^{\text{STB}}, P_i^{\text{WRM}}, P_i^{\text{min}}\}$
$J^{\text{HL}} = \{0, P_i^{\text{STB}}, P_i^{\text{min}}\}$
$\bar{J}^{\text{LL}} = \{0, P_i^{\text{CLD}}, P_i^{\text{STB}}, P_i^{\text{WRM}}, P_i^{\text{max}}\}$
$\bar{J}^{\text{HL}} = \{0, P_i^{\text{STB}}, P_i^{\text{max}}\}$
$P^{\text{LL}} = \{(0,0), (P_i^{\text{CLD}}, P_i^{\text{CLD}}), (P_i^{\text{STB}}, P_i^{\text{STB}}), (P_i^{\text{WRM}}, P_i^{\text{WRM}}), (P_i^{\text{min}}, P_i^{\text{max}})\}$
$P^{\text{HL}} = \{(0,0), (P_i^{\text{STB}}, P_i^{\text{STB}}), (P_i^{\text{min}}, P_i^{\text{max}})\}$
$G = \{\text{sale}, \text{pur}\}$

In the deliverable, formulations are derived in a discrete time k. The continuous time t can be obtained via $t = kT_s$, with T_s being the sampling time. This is important to highlight here that the superscripts IM, RM, HL, LL refer to intraday market, real-time market, high-level control and low-level control, respectively. For the sake of simplicity, and to achieve better readability, we will not use such superscripts unless in minor circumstances when ambiguities may arise.

3 System Description

The main components of the scenario under investigation are the wind generation unit, the hydrogen-based storage and generation system (electrolyzer, hydrogen tank and fuel cell), the hydrogen load, the grid, and the control and communication systems. For the sake of completeness, the scenario under investigation is depicted in Figure 1. The green solid lines denote energy flows, the blue lines show hydrogen flows and the red dashed lines denote data

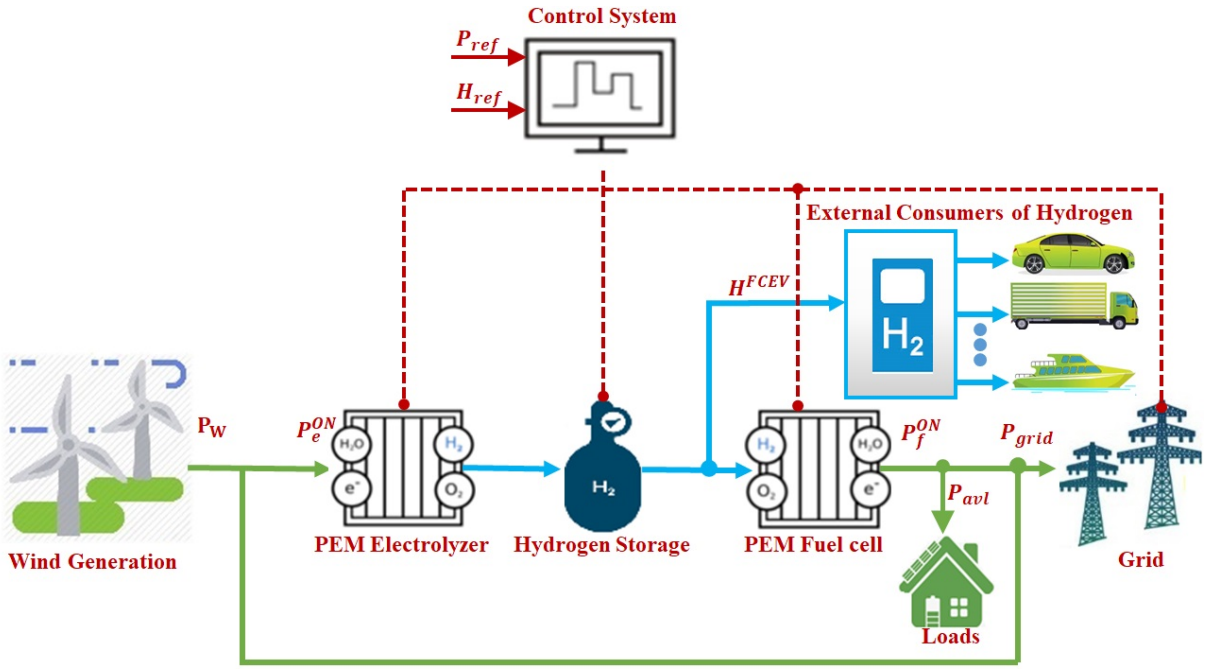

Figure 1: Scenario under investigation. P_e^{ON}, P_f^{ON}, P_W, P_{avl} and P_{grid} are the electrolyzer input power, the fuel cell output power, the wind power, the available system power and the grid power, respectively.

flows. Accordingly, P_w is the power generated by the wind farm, P_e^{ON} is the input power of the electrolyzer, P_f^{ON} indicates the output power of the fuel cell, H_{ref} is the hydrogen reference demand, P_{grid} is the grid exchanged power and P_{ref} is the load reference demand which has to be tracked by P_{avl}. It is important to highlight here that the possible exchange power with the grid is selling only.

4 General Operations

The control strategy developed under fuel production use cases has to fulfill two tasks:

1. to meet hydrogen demand for the road vehicles;
2. to sell energy to the grid through electrical market participation and to supply a local load after any excess of renewable generation has met the hydrogen demand.

Such objectives are pursued assuming two time-scales across which the relevant dynamics take place. A larger time-scale addresses the control objectives on daily basis, i.e., the controller has to allocate the optimal amount of hydrogen to be sold to FCEVs based on the day-after expected aggregate demand. Then, based on such allocation, all the extra hydrogen achieved via the wind-power conversion can be sold to the market to maximize the profit or used to supply a local load. A smaller time-scale addresses the deviations due to the inherent unreliability of the forecasts used for the larger time-scale. However, the smaller time-scale addresses only the market participation and the local load supply. In the larger time-scale, we prioritize

the optimization by firstly computing the optimal hydrogen level in the tank so as to track the FCEV's day-after expected demand, and then the optimal level is used as a constraint in a second optimization stage where the electrical market participation and the local load demand satisfaction are considered.

The block diagram of the proposed multi-level controller is shown in Figure 2. The low-level

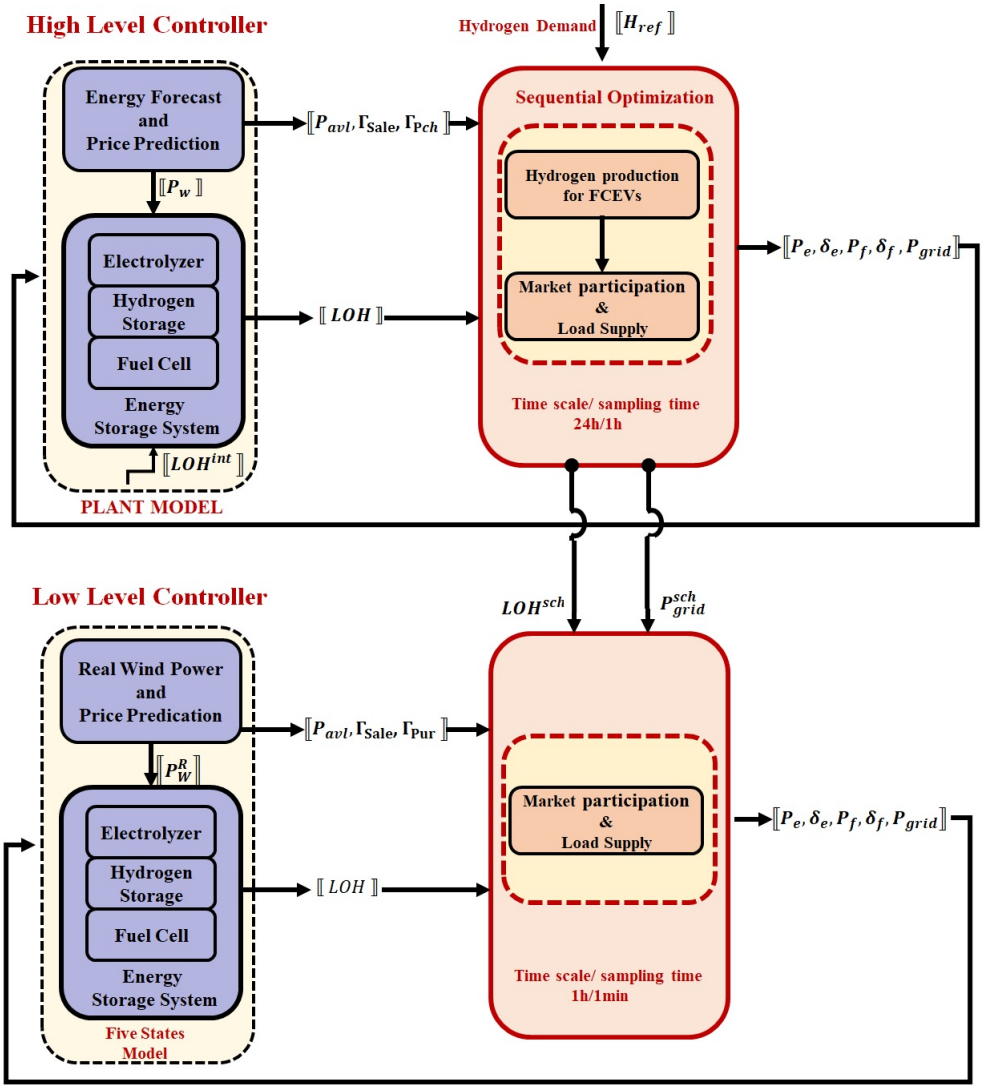

Figure 2: Multi-level Cascaded MPC Control Blockdiagram.

control will execute every 1 min with a scheduled horizon of 1 hr with 1 min sampling time and the high-level control will execute every 1 hour with a scheduled horizon of 24 hrs and 1 hour sampling time.

5 Control Design for Fuel-production Use Cases

This section describes the formulation of the control strategy presented in this deliverable. Each control level horizon explains the corresponding time-scale. We refer the reader to D6.1 [1] for the details on the formulation of the mathematical models used by the high-level controller and briefly reported in the following for the sake of completeness.

5.1 Mathematical Models for High-level Control

The mathematical models for high-level control are meant to enable the corresponding optimizer to achieve an optimal scheduling of the devices' operations according to forecasts. They basically provide what we agree to call a long-term plan about which the real-time strategy is very much likely to be found. For this reason, detailed logic models are not required at this stage that, therefore, will include only on, off and standby operations. We refer the reader to D6.1 [1] for the details on the formulation of the mathematical models used by the high-level controller and briefly reported in the following for the sake of completeness.

5.1.1 Electrolyzer and Fuel Cell Models

The mathematical models for the operations of the electrolyzer and the fuel cell over the larger time-scales, i.e., those addressed by the high-level control, consist of the corresponding three states automata, as also already adopted in previous deliverables. The automata are shown in Figure 3. For each one of them, the three states ON, OFF and STB are considered. Then, the mutually exclusive logical variables $\delta_i^a(k)$, are used to indicate the corresponding operating conditions at any time-step k. More in detail, each operational state of the electrolyzer

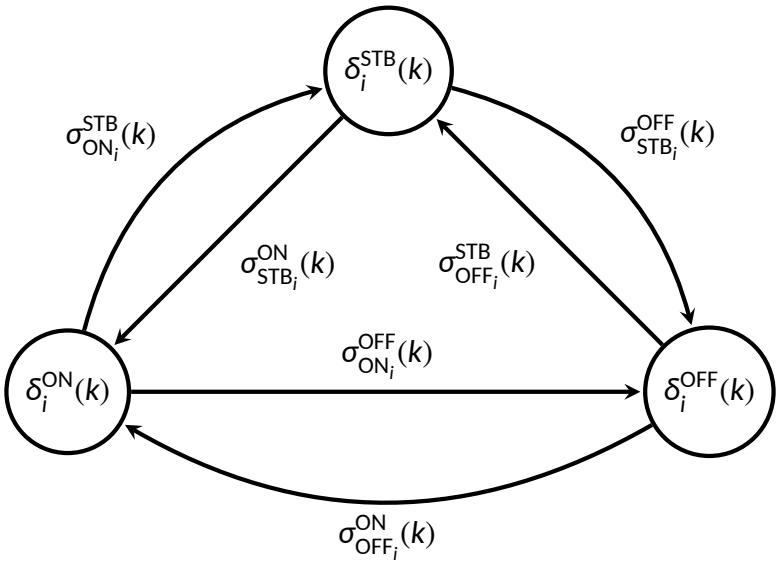

Figure 3: Automata of the electrolyzer ($i = e$) and of the fuel cell ($i = f$). Each node represents a particular state (i.e., operational mode), while the edges represent the state transition.

and the fuel cell results in a particular product of one logical variable and one correspond-

ing power, which is relevant for that state, to be different from zero. For example, whenever the electrolyzer is in ON state, the corresponding input power is limited within the range $[P_e^{\min}, P_e^{\max}]$. Thus, by defining $P_e(k)\delta_e^{\text{ON}}(k) = P_e^{\text{in}}$ and since in this case we set $\delta_e^{\text{ON}}(k) = 1$, it results $P_e(k) = P_e^{\text{in}} \in [P_e^{\min}, P_e^{\max}]$. Similar considerations can be carried out for the other states.

Along with the logical states, also the feasible state transitions $\sigma_{\alpha,i}^{\beta}(k)$ are part of the model and which can be defined by suitably combining the logical states through logical connectives. Both state variables and transition variables are codified with mixed-integer inequalities which are included as constraints into the MPC controller. The mathematical formulation of these constraints is reported, for the reader's convenience, in Appendix A. We also refer the reader to deliverable D6.1 for more insightful details.

5.1.2 Hydrogen Level Dynamics

The hydrogen level dynamics are similar to those considered in the other use cases except that in the fuel-production use case we introduce a loss term $H^{\text{FCEV}}\delta_{\text{FCEV}}$ which models the use of the stored hydrogen for supplying demand from fuel cell electric vehicles:

$$H(k+1) = H(k) - H^{\text{FCEV}}\delta_{FCEV}(k) + \eta_e P_e(k)\delta_e^{\text{ON}}(k)T_s - \frac{P_f(k)\delta_f^{\text{ON}}(k)T_s}{\eta_f}. \tag{1}$$

Notice that, according to (1) the electrolyzer and the fuel cell, respectively, produce and consume hydrogen only in their ON modes. Further, it may also happen that the electrolyzer and the fuel cell can be on at the same time. If this may result incoherent for any reasonable rationale, actually the corresponding degree of freedom will help the controller to minimize the switching costs, e.g., by keeping on the fuel cell whenever the previous switching happened "few" times before even if the electrolyzer is required to switch on.

5.1.3 Interaction with the Utility Grid

In the scenario under investigation, the energy can be sold to the grid. The selling of the energy after meeting the hydrogen demand is beneficial in achieving greater revenue generation. One state for power sale with the grid is expressed by the introduction of the logical variable $\delta^{\text{grid}}(k)$ whose activation ($\delta^{\text{grid}}(k)$=1) or deactivation ($\delta^{\text{grid}}(k) = 0$) depends on the interaction with the grid. Accordingly, the following transformation is done

$$[\delta^{\text{grid}}(k) = 1] \iff [P_{\text{grid}}(k) \geq 0], \tag{2}$$

which results in the inequality constraints

$$\begin{aligned} P_{\text{grid}}(k) &\geq m^{\text{grid}}(1 - \delta^{\text{grid}}(k)), \\ P_{\text{grid}}(k) &\leq (M^{\text{grid}} + \epsilon)\delta^{\text{grid}}(k) - \epsilon, \end{aligned} \tag{3}$$

where $m^{\text{grid}} < 0$ and $M^{\text{grid}} > 0$ are a lower bound and an upper bound of the function $P_{\text{grid}}(k)$, respectively, and ϵ is a suitably small positive constant[1]. Starting from the definition of the

[1] ϵ is typically the machine precision which in our case is equal to $\epsilon = 2.2204e^{-16}$.

logical variable $\delta_{\text{grid}}(k)$ in (2), the auxiliary variables $P^{\text{sale}}(k)$ can be defined as

$$P^{\text{sale}}(k) = -P_{\text{grid}}(k)(1 - \delta^{\text{grid}}(k)). \tag{4}$$

The variable $P^{\text{sale}}(k)$ hides a non-linearity and models the selling events to the utility grid. The mixed-integer product of (4) cannot be directly handled by numerical solvers and, therefore, a further manipulation is needed. The variables defined above in (2) and (4) can be expressed as mixed-logic inequalities. Then, the selling microgrid behavior can be recast as

$$\begin{aligned} P^{\text{sale}}(k) &\leq m^{\text{grid}}(\delta^{\text{grid}}(k) - 1), \\ P^{\text{sale}}(k) &\geq M^{\text{grid}}(\delta^{\text{grid}}(k) - 1), \\ P^{\text{sale}}(k) &\geq -P_{\text{grid}}(k) + m^{\text{grid}}\delta^{\text{grid}}(k), \\ P^{\text{sale}}(k) &\leq -P_{\text{grid}}(k) - M^{\text{grid}}\delta^{\text{grid}}(k). \end{aligned} \tag{5}$$

The technique adopted for transforming the (nonlinear) mixed product in (2) in the equivalent mixed-linear formulation (5) can be analogously used for the other mixed products occurring in this manuscript. To keep the paper easy to be read, the repetition of such transformation has not been reported for other analogous cases later in the deliverable.

5.1.4 Power Balance Constraints

The power balance between energy production and consumption must be reached at each time-step k; hence the following equality constraint holds

$$P_w(k) - P_e(k)\delta_e^{\text{ON}}(k) + P_f(k)\delta_f^{\text{ON}}(k) - P_{\text{avl}}(k) = P_{\text{grid}}, \tag{6}$$

where $P_e(k)\delta_e^{\text{ON}}(k) = P_e^{\text{in}}$ and $P_f(k)\delta_f^{\text{ON}}(k) = P_f^{\text{out}}$. For the sake of generality of the modeling, such feature has therefore been included in the power balance equation.

5.1.5 Physical and Operating Constraints

The system physical and operating constraints, i.e., ramp up constraints, and hydrogen storage tank constraints have been taken into account in MPC control. We refer the reader to D6.1 and D6.2 for the detailed understanding of these constraints formulation.

5.1.6 High-Level MPC Design

The purpose of the high-level control is to provide a strategy based on forecasts. At this level, the controller handles hydrogen production for FCEVs, the local load tracking and the energy market participation. However, hydrogen production has the highest priority, therefore the optimal scheduling of hydrogen production and re-electrification are solved sequentially. Firstly, the hydrogen forecast demand for FCEV is addressed through the minimization of the quadratic deviation from the expected hydrogen demand. Then, the optimal level of hydrogen is used as a constraint in the second stage where the load tracking and the market participation are addressed. Of course, the operating costs are also minimized as well as the systems and application requirements are fulfilled through appropriate constraints as usual. In what follows, the cost functions will be defined with respect to the implementation within an MPC scheme, i.e., where, for a given time-step k, they will be minimized $j = 0, \dots, T-1$ steps ahead.

5.1.7 Operating Cost Function

The cost functions that model the electrolyzer and the fuel cell operating costs include several terms accounting for the component depreciation, the reduction of life cycles, the energy spent in keeping the units warm during standby, the energy spent for cold start and the energy spent for the warm start. The fluctuating loads and the operating cycles can seriously affect these devices in a number of ways. Therefore, in order to tackle such problems, we propose the following cost functions

$$\begin{aligned} J_i^{\mathrm{HL}}(k+j) = &\left(\frac{S_{\mathrm{rep},i}}{\mathrm{NH}_i} + \mathrm{C}_i^{\mathrm{OM}}\right)\delta_i^{\mathrm{ON}}(k+j) \\ &+ \mathrm{C}_{\mathrm{OFF},i}^{\mathrm{ON}}\sigma_{\mathrm{OFF},i}^{\mathrm{ON}}(k+j) \\ &+ \mathrm{C}_{\mathrm{ON},i}^{\mathrm{OFF}}\sigma_{\mathrm{ON},i}^{\mathrm{OFF}}(k+j) \\ &+ \mathrm{C}_{\mathrm{ON},i}^{\mathrm{STB}}\sigma_{\mathrm{ON},i}^{\mathrm{STB}}(k+j) \\ &+ \mathrm{C}_{\mathrm{STB},i}^{\mathrm{ON}}\sigma_{\mathrm{STB},i}^{\mathrm{ON}}(k+j) \\ &+ \mathrm{C}_{\mathrm{STB},i}^{\mathrm{OFF}}\sigma_{\mathrm{STB},i}^{\mathrm{OFF}}(k+j) \\ &+ \mathrm{C}_{\mathrm{OFF},i}^{\mathrm{STB}}\sigma_{\mathrm{OFF},i}^{\mathrm{STB}}(k+j) \\ &+ s(k+j)P_i^{\mathrm{STB}}\delta_i^{\mathrm{STB}}(k+j), \end{aligned} \tag{7}$$

where NH_i is the number of life hours of the electrolyzer and of the fuel cell, $\mathrm{C}_i^{\mathrm{OM}}$ denotes the operating and maintenance cost of the electrolyzer and the fuel cell, $s(k)$ is the power spot price. $\mathrm{C}_{\mathrm{OFF},i}^{\mathrm{ON}}$, $\mathrm{C}_{\mathrm{ON},i}^{\mathrm{OFF}}$, $\mathrm{C}_{\mathrm{STB},i}^{\mathrm{ON}}$, $\mathrm{C}_{\mathrm{ON}_i}^{\mathrm{STB}}$, $\mathrm{C}_{\mathrm{STB}_i}^{\mathrm{OFF}}$, and $\mathrm{C}_{\mathrm{OFF}_i}^{\mathrm{STB}}$ describe the startup, shutdown and standby cost of the electrolyzer and the fuel cell, respectively choosing $i \in \{e, f\}$. These costs are paid any time a mode switch occurs, since the switchings result in reduction of the working cycle and, therefore, reduce the components' life. We wish to emphasize, for the sake of clarity, that shifting from OFF to ON (cold start) presents usually a higher cost than from STB to ON (warm start). On the other hand, devices in OFF mode do not absorb any power, while this is not true in STB mode. The $S_{\mathrm{rep},e}$ and $S_{\mathrm{rep},f}$ represent the stack replacement cost of the electrolyzer and that of the fuel cell, respectively.

5.1.8 Intraday Market Cost Function

The cost function explains the selling energy to the grid through electrical market participation and is given by

$$J_g^{\mathrm{HL}}(k+j) = -\Gamma^{\mathrm{sale}}(k+j)P_{\mathrm{sale}}^{\mathrm{HL}}(k+j)T_s, \tag{8}$$

where Γ^{sale} are the energy price profiles in [€/kWh]. Power sale within the grid is expressed by the introduction of logical state $\delta^{\mathrm{grid}}(k)$, as explained in Sec. 5.1.3.

5.1.9 Local Load Tracking Cost Function

One control goal of the proposed controller is the tracking of a local load demand P_{ref}. To achieve this, the controller will also minimize the cumulative squared error between P_{ref} and

P_{avl}:

$$J_l^{\text{HL}}(k+j) = \Big(P_{\text{avl}}(k+j) - P_{\text{ref}}(k+j)\Big)^2. \tag{9}$$

5.1.10 Hydrogen Demand Tracking Cost Function

One goal of the controller is to track the exchange process demand H^{ref} with the final exchange of hydrogen delivered by the microgrid H^{FCEV}. To this aim, the reference tracking cost function is given by the cumulative squared error between H^{ref} and H^{FCEV} as follows

$$J_{\text{FCEV}}^{\text{HL}}(k+j) := \Big(H^{\text{FCEV}}(k+j)\delta_{\text{FCEV}}(k+j)\Big) - H^{\text{ref}}(k+j)\Big)^2. \tag{10}$$

5.1.11 Sequential MPC Scheme

In order to comply with the fuel-production use case as specified in the IEA-HIA Task 24 Final Report [4], hydrogen production has the highest priority among all the other control objectives. As introduced, the high-level controller addresses time scales of the order of one day with a sampling time of 1 hour. At such time scales, the relevant objectives, in addition to hydrogen production, are the energy supply to the local load and the market participation, which both have lower priority. The identified order suggests then to sequentially operate the optimization, where firstly the hydrogen production amount is scheduled based on the expected (forecast) aggregated hydrogen demand of the next day. The computed optimal hydrogen level in the tank is then introduced as a constraint in the second optimization stage where the load tracking and the market participation are addressed at the same time through a linear combination of the corresponding cost functions. Let us now introduce the set $\mathscr{C}$ of all the decision variable vectors defined as

$$\mathscr{C}_k := \Big\{\boldsymbol{P}_{\text{i},k}^{T-1}, \boldsymbol{P}_{\text{avl},k}^{T-1}, \mathbf{P}_{w,k}^{T-1}, \boldsymbol{\delta}_{\text{i},k}^{\alpha,T-1}, \boldsymbol{\sigma}_{\alpha,\text{i},k}^{\beta,T-1}, \boldsymbol{z}_{i,k}^{\geq\gamma,T-1}, \boldsymbol{z}_{i,k}^{\leq\bar{\gamma},T-1}, \boldsymbol{P}_{\text{grid},k}^{T-1}\Big\}. \tag{11}$$

In other words, the problem is recast as

$$\begin{aligned}
\underset{\mathscr{C}_k}{\text{minimize}} \quad & \sum_{j=0}^{T-1} \rho_l J_l(k+j) + \rho_g J_g(k+j) + \rho_e J_e(k+j) + \rho_f J_f(k+j) \\
\text{subject to} \quad & (1), (5), (6), (22), (23), (25), \\
& H \geq H^*, \\
& \delta_i^\alpha, \delta_{\alpha_i}^\beta \in [0,1] \qquad \alpha, \beta \in \{\text{OFF}, \text{ON}, \text{STB}\}, \alpha \neq \beta, \\
& z_i^{\geq\gamma}, z_i^{\leq\bar{\gamma}} \in \{0,1\} \qquad (\gamma, \bar{\gamma}) \in \{(0,0), (P_i^{\min}, P_i^{\max}), (P_i^{\text{STB}}, P_i^{\text{STB}})\}.
\end{aligned} \tag{12}$$

where

$$\begin{aligned}
H^* = \underset{\mathscr{C}_k}{\arg\min} \quad & \sum_{j=0}^{T-1} J_{\text{FCEV}}(k+j) \\
\text{subject to} \quad & (1), (5), (6), (22), (23), (25), \\
& \delta_i^\alpha, \delta_{\alpha_i}^\beta \in [0,1] \qquad \alpha, \beta \in \{\text{OFF}, \text{ON}, \text{STB}\}, \alpha \neq \beta, \\
& z_i^{\geq\gamma}, z_i^{\leq\bar{\gamma}} \in \{0,1\} \qquad (\gamma, \bar{\gamma}) \in \{(0,0), (P_i^{\min}, P_i^{\max}), (P_i^{\text{STB}}, P_i^{\text{STB}})\}.
\end{aligned} \tag{13}$$

where T is the simulation horizon and ρ_l, ρ_g, ρ_e and ρ_f are the weights of the load tracking, grid participation, electrolyzer operating and fuel cell operating cost functions, respectively, that can be tuned so as to achieve a desired prioritization among them. The complete formulations of (12)–(13) is reported, for the reader's convenience, in Appendix A.4.

5.2 Mathematical Models for Low-level Control

This section presents the mathematical models and the MPC formulation to solve real-time electrical market participation and to track the load demand after any excess of renewable generation has met the forecast hydrogen demand at high-level. The low-level MPC controller receives the references scheduled by the high-level MPC , i.e. LOH_{sch}, P^{e}_{sch}, P^{f}_{sch}, and $P^{\text{grid}}_{\text{sch}}$ and use them for the optimization of the real-time operations as will be clearer later. The low-level control will execute every 1 minute with a scheduled horizon of 1 hour and sampling time of 1 min. We refer the reader to D6.2 [2] for the details on the formulation of the mathematical models used by the low-level controller and briefly reported in the following for sake of completeness.

5.2.1 Electrolyzer and Fuel Cell Models

The mathematical models for the operations of the electrolyzer and the fuel cell over a shorter prediction horizon and faster sampling, i.e., those addressed by the low-level control, consist of corresponding five states automata, as shown in Figure 4. The two states CLD and WRM are actually virtual states since a device can be in one of them for a limited time interval.

Figure 4 shows also the mode transitions that the electrolyzer and the fuel cell can undergo. It is important to highlight that the transitions affecting the operating costs are between the states ON–OFF, CLD–STB and STB–OFF with considerations similar to those in Sec. 5.2.7. Also in this case, electrolyzer and fuel cell models depending on logical variables and state transitions are achieved. Then, they are codified with mixed-integer linear inequalities which will be then included as constraints for the low-level MPC controller. The mathematical formulation of the constraints is reported, for the reader's convenience, in Appendix B. We also refer the reader to deliverable D6.2 [2] where the same approach in a similar scenario has been also presented.

5.2.2 Hydrogen Level Dynamics

The hydrogen level dynamics for the low-level controller are modeled with similar equations to those used for the high-level controller in Sec. 5.1.2, providing that the logic variables refer to the corresponding models used by the low-level controller and $T_s = 1$ min.

5.2.3 Interaction with the Utility Grid

The detailed grid MLD formulation for the real-time market grid cost function has been done with the introduction of logical and dynamic variables. The resulting equations are similar to those developed in Sec. 5.1.3 for the high-level controller with minor exceptions due to the

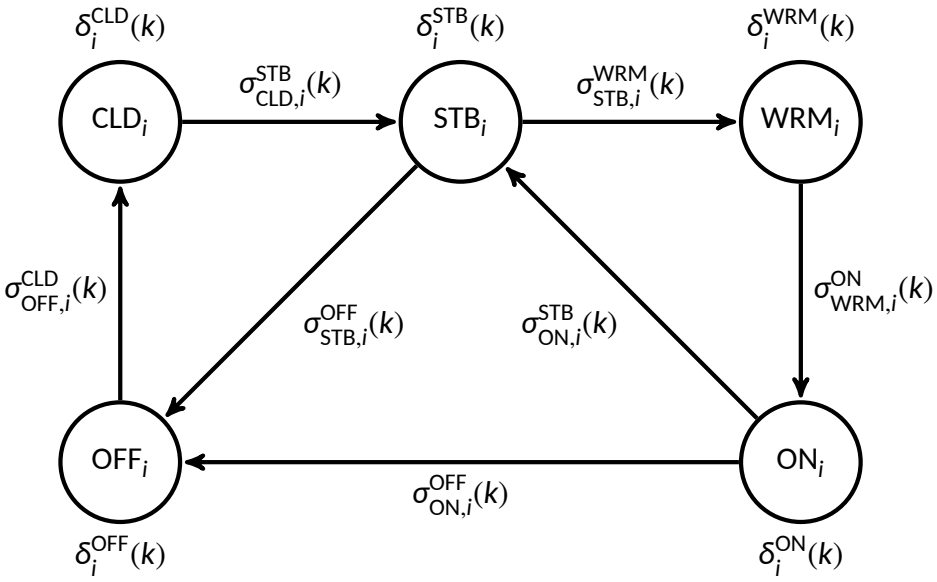

Figure 4: Operational modes sequential graph of the *i* device.

different time scales and the connections between the models of the two levels. The reader can refer to Appendix B.5 for details.

5.2.4 Power Balance Constraints

The power balancing equation has been modeled and formulated with similar equations used for high-level control providing that all the relevant variables have to be referred to the low-level and $T_s = 1$ min.

5.2.5 Physical and Operating Constraints

The system operating and physical constraints i.e., ramp up/down constraints have been modeled and formulated with similar equations used for high-level control providing that all the relevant variables have to be referred to the low-level and $T_s = 1$ min.

5.2.6 Low-Level MPC Design

The real-time MPC controller helps to match generation and load within time ranges of the order of minutes. There is a penalty deviation cost used as an incentive for the real-time market participants to maintain their power balance. The importance of the reference levels marked for the ESS in every hour by the previous MPC controllers must be taken into account. The sample time of the low-level MPC is 1 min, while its scheduled horizon 1 hour. In order to avoid further deviations in these instants after this controller schedule, the final references for the level of stored energy have to be followed.

The low-level MPC receives as references the scheduling of the electrolyzer, fuel cell and grid powers, from the high-level MPC, which addresses larger time-scales. In what follows,

we use the two time-steps k and m, where k refers to the high-level and m to the low-level, in order to highlight the link between the cost functions at low-level and the two time-scales. An additional time-step p is used at low-level time-scales so as to define the low-level cost functions implementation within an MPC scheme, similarly to what done for the high-level (see Sec.5.1.6).

5.2.7 Operating Cost Function

The economical dispatch of the microgrid gives both references to the schedule in energy and in power at each instant. The operating cost of the use of hydrogen ESS for the low-level MPC is a penalty from the final instant of the control horizon combined with the aspects of degradation and useful cost of this system

$$\begin{aligned} J_i^{\mathrm{LL}}(k, m+p) \; := & \left(\frac{S_{\mathrm{rep,i}}}{\mathrm{NH}_i} + C_{\mathrm{i}}^{\mathrm{OM}} \right) \delta_{\mathrm{i}}^{\mathrm{ON}}(k, m+p) \\ & + C_{\mathrm{ON_i}}^{\mathrm{OFF}} \sigma_{\mathrm{ON_i}}^{\mathrm{OFF}}(k, m+p) \\ & + C_{\mathrm{CLD_i}}^{\mathrm{STB}} \sigma_{\mathrm{CLD}_i}^{\mathrm{STB}}(k, m+p) \\ & + C_{\mathrm{STB_i}}^{\mathrm{OFF}} \sigma_{\mathrm{STB_i}}^{\mathrm{OFF}}(k, m+p) \\ & + c(k) P_{\mathrm{i}}^{\mathrm{STB}} \delta_{\mathrm{i}}^{\mathrm{STB}}(k, m+p) \\ & + c(k) P_{\mathrm{i}}^{\mathrm{CLD}} \delta_{\mathrm{i}}^{\mathrm{CLD}}(k, m+p) \\ & + c(k) P_{\mathrm{i}}^{\mathrm{WRM}} \delta_{\mathrm{i}}^{\mathrm{WRM}}(k, m+p) \\ & + \omega_{\mathrm{tank}}^{E} \left(H^{LL}(k, m+p) - H^{HL}(k) \right)^2 \\ & + \sum_{\alpha \in A} \omega_{\mathrm{i}}^{P} \left(P_{\mathrm{i}}^{LL,\alpha}(k, m+p) \delta_{\mathrm{i}}^{LL,\alpha}(k, m+p) - P_{\mathrm{i}}^{HL,\alpha}(k) \delta_{\mathrm{i}}^{HL,\alpha}(k) \right)^2, \end{aligned} \tag{14}$$

where $\omega_{\mathrm{tank}}^{E}$ is the weighting factor for the deviation in energy stored in the hydrogen tank for low-level control with respect to the energy schedule given in the high-level control, ω_{i}^{P} are the terms to penalize the power deviation of the electrolyzer and the fuel cell from their high-level control scheduled power. The power spot price, the devices' transitions and the costs related to them have been considered the same providing in the high-level control devices operating cost functions.

5.2.8 Real-time Market Cost Function

Due to the high penalties imposed by the system operator in the real-time market, the tracking deviation of the power exchange with the main grid P_{grid} versus the contracted-schedule with the Market/System Operator is considered. The low-level MPC grid cost function is given by

$$J_{\mathrm{grid}}^{\mathrm{LL}}(k, m+p) \; := - \Gamma^{\mathrm{sale}}(k, m+p) P_{\mathrm{sale}}^{\mathrm{LL}}(k, m+p) T_s \tag{15}$$

where $\Gamma^{\mathrm{sale}}(k, m+p)$ is the real-time market profile. However, since in the Norwegian market the prices are actually given only on hourly basis, in the specific scenario targeted by HAEOLUS, $\Gamma^{\mathrm{sale}}(k, m) = \Gamma^{\mathrm{sale}}(k)$ for any m such that mT_s is within the low-level scheduling horizon for

any given k. Nonetheless, the addressing of the market participation in real-time introduces a further degree of freedom that the controller can exploit in order to achieve improved strategies during real-time operations. Power sale at the low-level MPC with the grid is expressed by the introduction of logical variables $\delta_{\text{grid}}(k,m)$. The detailed MLD formulation for the real-time market grid cost function has been done with the introduction of logical and dynamic variables and is reported in (41) of Appendix B.

5.2.9 Local Load Tracking Cost Function

For real-time operations, the local load tracking is achieved through the minimization of

$$J_l^{\text{LL}}(k,m+p) = \left(P_{\text{avl}}^{\text{LL}}(k,m+p) - P_{\text{ref}}(k)\right)^2 + \lambda_\epsilon \epsilon \tag{16}$$

where $k \in \{1,\dots,24\}$ is the high-level MPC index, and λ_ϵ is a penalty factor introduced to minimize ϵ rapidly. Since there is not an energy forecast model, the controller uses directly the real-time measurements (generation and consumptions) to calculate the real-time market available power P_{avl}. The controller assumes that these values are going to be constant during the prediction horizon. The double references (forecast and real-time) gives a degree of freedom in the controller to correct power deficit scenario with an exceeding scenario, and in order to achieve this, (16) must be considered with the following additional constraint

$$P_{\text{avl}}^{\text{LL}}(k,m+p) - P_{\text{avl}}^{\text{HL}}(k) \leq \epsilon. \tag{17}$$

Let us define the global cost function of the real scenario to be minimized by the low-level MPC controller as

$$J^{\text{LL}}(k,m) = \sum_{p=1}^{\text{SH}} \left(\rho_{\text{grid}} J_{\text{grid}}^{\text{LL}}(k,m+p) + \rho_l J_l^{\text{LL}}(k,m+p) + \rho_e J_e^{\text{LL}}(k,m+p) + \rho_f J_f^{\text{LL}}(k,m+p)\right), \tag{18}$$

where ρ_l, ρ_e,ρ_f and ρ_{grid} are the weighting factors for dimensionless analysis of the low-level control cost function. In the next subsections, (18) will be particularized for the ESS.

5.2.10 MPC Scheme

This subsection explains the low-level MPC formulation for the participation of the electricity market to maximize the revenue generations and load tracking. Let us now introduce the set $\mathscr{C}$ of all the decision variable vectors defined as

$$\mathscr{C}_{k,m} := \left\{\boldsymbol{P}_{\text{i},k,m}^{T-1}, \boldsymbol{P}_{\text{avl},k,m}^{T-1}, \boldsymbol{P}_{w,k}^{T-1}, \boldsymbol{\delta}_{\text{i},k,m}^{\alpha,T-1}, \boldsymbol{\sigma}_{\alpha,\text{i},k,m}^{\beta,T-1}, \boldsymbol{z}_{i,k,m}^{\geq\gamma,T-1}, \boldsymbol{z}_{i,k,m}^{\leq\bar{\gamma},T-1}, \boldsymbol{P}_{\text{grid},k,m}^{T-1}\right\}. \tag{19}$$

For any given pair (k,m), the MPC problem for the low-level control is

$$\begin{aligned}
\underset{\mathscr{C}_{k,m}}{\text{minimize}} \quad & J^{\text{LL}}(k,m) \\
\text{subject to} \quad & (33),(34),(36)-(39),(41), \\
& \delta_i^\alpha, \delta_{\alpha_i}^\beta \in [0,1] \qquad \alpha,\beta \in \{\text{OFF},\text{ON},\text{STB},\text{CLD},\text{WRM}\}, \alpha \neq \beta, \\
& z_i^{\geq\gamma}, z_i^{\leq\bar{\gamma}} \in \{0,1\} \qquad (\gamma,\bar{\gamma}) \in \{(0,0),(P_i^{\min},P_i^{\max}),(P_i^{\text{STB}},P_i^{\text{STB}}), \\
& \qquad\qquad (P_i^{\text{CLD}},P_i^{\text{CLD}}),(P_i^{\text{WRM}},P_i^{\text{WRM}})\}
\end{aligned} \tag{20}$$

Since for any given k the problem (44) is solved again at time instants $m+1, \ldots, m+p-1$, an optimal feedback strategy is generated and applied in real-time. The complete formulation of (44) is reported, for the reader's convenience, in Appendix B.6.

6 Results Analysis and Discussion

In order to present the effectiveness of the control algorithm for fuel production use cases, simulations under stressing plant scenario over a 24 hours horizon have been performed. It is important to highlight here that the contribution of the implemented algorithm is to control the hydrogen-based ESS so as to enable the wind farm to operate conforming to the fuel production use cases [4] as per the project goals [5].

To prove the efficacy of the proposed multi-layer MPC, two scenarios have been achieved. In the first scenario, equal weight choices for the tracking of the local load demand and the participation to the energy market have been assigned. In the second scenario, the weights are changed, that is one sets greater than the other, and vice versa. Of course, in both scenarios, the fulfillment of the hydrogen demand has the highest priority.

6.1 Hydrogen demand satisfaction

Figure 5 reports several profiles. In particular, Figure 5(a) reports the power generated by the wind farm, Figure 5(b) reports the hydrogen level in the tank, the hydrogen reference demand and the hydrogen scheduling as provided by the high-level controller, Figure 5(c) shows the load demand profile and the power available as scheduled by the high-level controller and Figure 5(d) shows the power the high-level controller allocate for the grid market participation and the energy market price profile. From Figure 5(b), it can be observed that the hydrogen demand is met in all 24 hours of the day. Figure 5(c) shows that also the local load reference demand is met as per the availability of hydrogen in the tank. Figure 5(d) shows the selling policy of the high-level controller for the energy market participation against the price profiles. Interestingly, from 19-20 hours, the controller decides not to sell electricity to the market even though the prices are increasing. However, thanks to this decision, the load demand is met and the hydrogen level in the tank is also able to increase so as to comply with the future operations. This is compatible with the choice of equal weights for the load demand tracking and the market participation cost functions, and shows also the kind of nontrivial decisions that can be addressed by the developed algorithm. Figure 6 shows the low-level policy, i.e. that which is actually implemented by the algorithm, and the evolution of the hydrogen level in the tank in reality (Figure 5(b)). In particular, such level takes also into account the hydrogen that is provided to the electric vehicles, that is, the profile shown in the picture is only the profile available for the load demand tracking and the energy market participation, which are shown in Figure 6(c), Figure 6(d). The implemented strategy is such that, sometimes, the load demand is not met and the controller decides not to sell electricity to the market. However this in compliance with the objective of the fuel cell use case where other additional objectives than the provision of hydrogen to FCEVs can be considered as optional features and not strict requirements. Another point to remark is that, even though we have assumed same wind generation, load demand and market price profiles for the high-level (forecasts) and for the

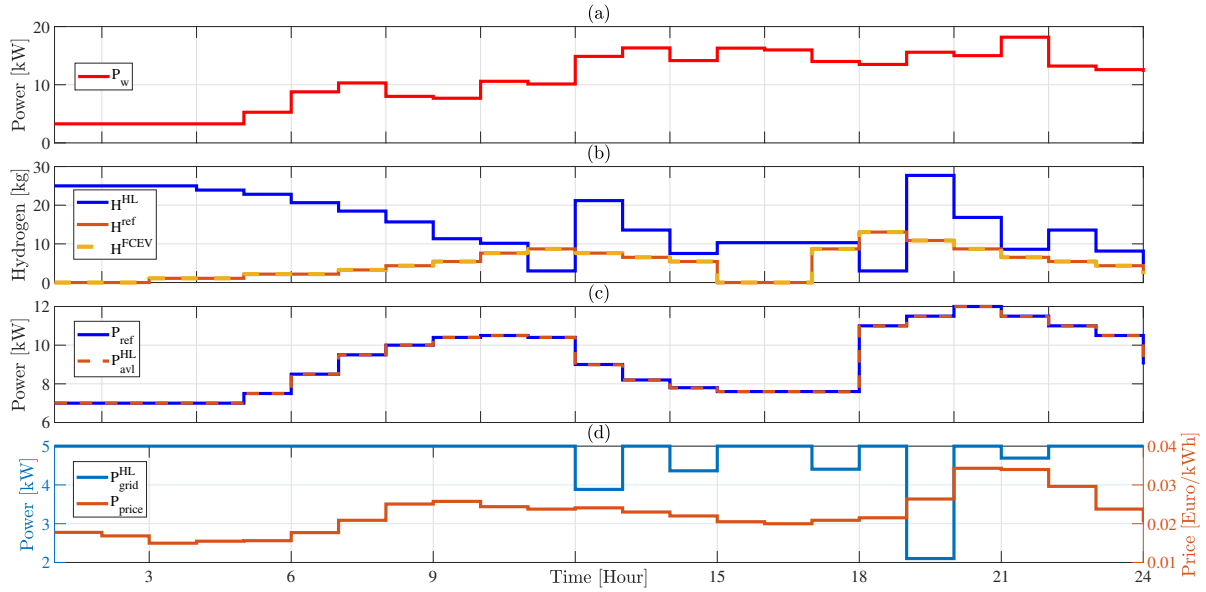

Figure 5: Profiles : (a) Wind power profile. (b) Hydrogen level H^{HL} and hydrogen demand tracking between H^{ref} and H^{FCEV}.(c) Load demand tracking between P_{ref} and P^{HL}_{avl}. (d) Shelling power and intraday market profile.

low-level control (real data), the low-level policy actually implemented by the controller, is very different from that of the high-level, especially in the market participation. This difference can be explained by the fact that the operating cost functions of the high- and low-level are different since, e.g., at high-level three states automata are used while at low-level five states automata are used in order to take into account also for cold and warm starts. Further, not all the transitions are enabled for the five states automata.

A comparison between the high-level and the low-level policies and evaluations of the relevant parameters are given in Figure 7.

6.2 Controller behaviour for different weights

This subsection shows how the the weight factors associated with the energy market and local load cost functions affect the operations of the system. The same wind power generation, local load reference demand and market profile as used in the first scenario are used in order to ease the comparison.

Figure 8 shows different plots for $\rho_g > \rho_l$ and $\rho_g < \rho_l$. In particular, Figure 8(c) shows the different policies in the available power to the load that the control achieves, where P_{avl} in case of $\rho_g > \rho_l$ is decreased, e.g., between 8-10 hrs, w.r.t. that for the opposite choice of the weights. Figure 8(d) shows the interaction with the grid through electrical market participation. It is observable that when $\rho_g > \rho_l$, the solver gives priority to the energy market participation in order to maximize the revenues. During this scenario, the local load demand is given less priority, thus, resulting in non-compliance with the local load demand during the hours 8-11, as also mentioned before (see Figure 8(c)). Conversely, by setting $\rho_l > \rho_g$ will push the solver to give high priority in meeting the load demand with respect to selling energy to the grid. The

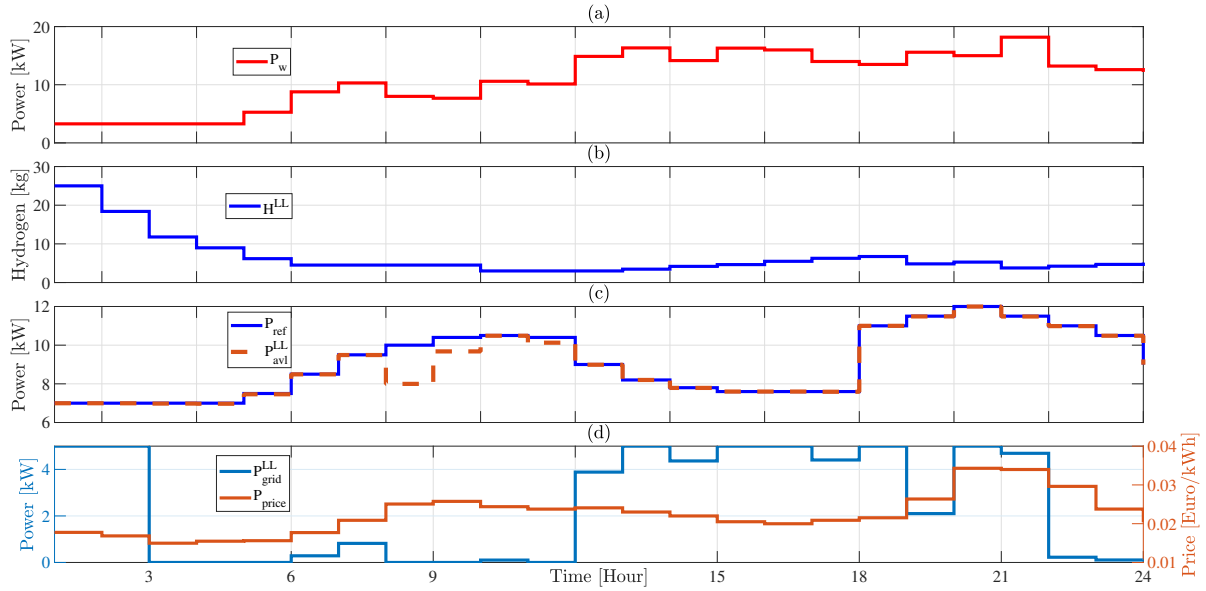

Figure 6: Low-level MPC controller: (a) Wind power profile. (b) hydrogen level H^{LL}. (c) Load demand tracking between P_{ref} and P^{LL}_{avl}. (d) Shelling power and real-time market profile.

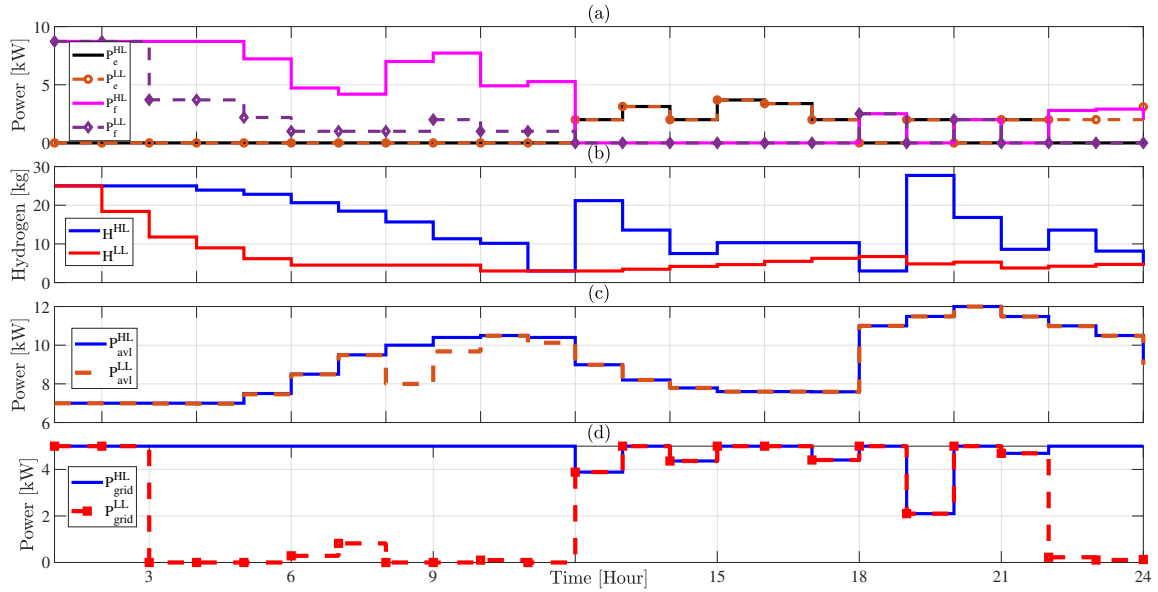

Figure 7: Control response of the system for two-layer: (a) Control response of the devices. (b) Control response of hydrogen storage. (c) Load demand tracking. (d) Control response of utility grid.

controller successfully tracked the load profile first, and then the remaining energy is sold to the grid.

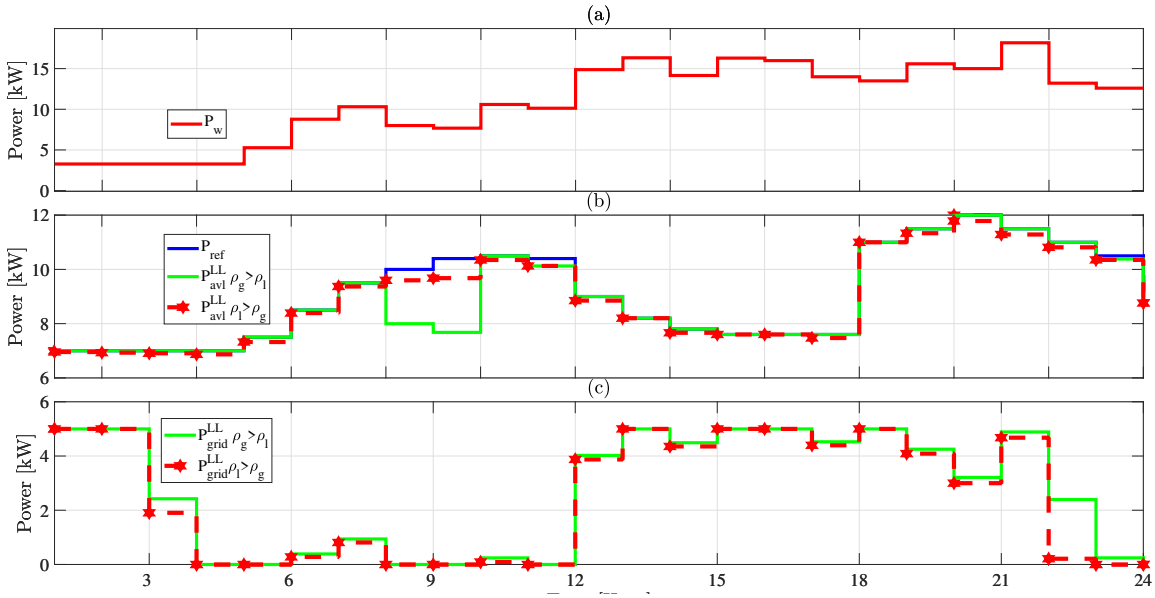

Figure 8: Controller behaviour for different weights: (a) Wind power. (b) Load demand tracking. (c) Control response of utility grid.

7 Conclusions

In this deliverable, we presented a hierarchical MPC approach for energy management of a wind farm equipped with a hydrogen storage system. The adoption of the multi-level MPC architecture allows to cope with the simultaneous satisfaction of hydrogen demand for the road vehicles along with the local electric and the contractual loads. In particular, at the first level, the larger time scale hydrogen market is addressed with the highest priority. In order to provide extra features, the local and contractual load satisfaction has also been considered in the control system. The low-level MPC receives and tracks the references computed by the high-level MPC, which helps in the correct implementation of the high-level policy based on forecasts.

References

[1] M. F. Shehzad, M. B. Abdelghany, D. Liuzza, and L. Glielmo, "Dynamic model for hydrogen production and storage plants," Deliverable D6.1, Public Deliverable, Tech. Rep. 779469, 2019, h2020-JTI-FCH-2017-1. [Online]. Available: https://www.haeolus.eu/?p=666

[2] M. B. Abdelghany, M. F. Shehzad, V. Mariani, D. Liuzza, and L. Glielmo, "Control system for energy-storage use case," Deliverable D6.2, Public Deliverable, Tech. Rep. 779469, 2020, h2020-JTI-FCH-2017-1. [Online]. Available: https://www.haeolus.eu/?p=876

[3] ——, "Control system for mini-grid use case," Deliverable D6.3, Public Deliverable, Tech. Rep. 779469, 2020, h2020-JTI-FCH-2017-1. [Online]. Available: https://www.haeolus.eu/?p=886

[4] "IEA-HIA task 24 wind energy & hydrogen integration," http://ieahydrogen.org/PUBLICATIONS,-REPORTS-PRESENTATIONS/Final-Reports-V2.aspx.

[5] HAEOLUS, "Hydrogen-Aeolic Energy with Optimized Electrolysers Upstream of Substatio Project," http://www.haeolus.eu/, accessed April 24, 2020.

[6] A. Bemporad and M. Morari, "Control of systems integrating logic, dynamics, and constraints," *Automatica*, vol. 35, no. 3, pp. 407–427, 1999.

A Appendix A

A.1 Intraday Market Constraints Formulation of the Logical States

In order to cope with an optimal control framework, we need to introduce 12 auxiliary Boolean variables $z_i^{\gamma}(k) \in \{0,1\}$, with $\gamma \in \{\geq 0, \leq 0, \geq P_i^{\text{STB}}, \leq P_i^{\text{STB}}, \geq P_i^{\min}, \leq P_i^{\max}\}$ and $i \in \{e,f\}$ [6]

$$z_i^{\geq 0}(k) = \begin{cases} 1 & P_i(k) \geq 0, \\ 0 & P_i(k) < 0, \end{cases} \tag{21a}$$

$$z_i^{\leq 0}(k) = \begin{cases} 0 & P_i(k) > 0, \\ 1 & P_i(k) \leq 0, \end{cases} \tag{21b}$$

$$z_i^{\geq P_i^{\text{STB}}}(k) = \begin{cases} 1 & P_i(k) \geq P_i^{\text{STB}}, \\ 0 & P_i(k) < P_i^{\text{STB}}, \end{cases} \tag{21c}$$

$$z_i^{\leq P_i^{\text{STB}}}(k) = \begin{cases} 0 & P_i(k) > P_i^{\text{STB}}, \\ 1 & P_i(k) \leq P_i^{\text{STB}}, \end{cases} \tag{21d}$$

$$z_i^{\geq P_i^{\min}}(k) = \begin{cases} 1 & P_i(k) \geq P_i^{\min}, \\ 0 & P_i(k) < P_i^{\min}, \end{cases} \tag{21e}$$

$$z_i^{\leq P_i^{\max}}(k) = \begin{cases} 0 & P_i(k) > P_i^{\max}, \\ 1 & P_i(k) \leq P_i^{\max}. \end{cases} \tag{21f}$$

Then, (21) can be expressed as

$$\begin{aligned} P_i(k) &< M z_i^{\geq 0}(k), \\ -P_i(k) &\leq M(1 - z_i^{\geq 0}(k)); \end{aligned} \tag{22a}$$

$$\begin{aligned} -P_i(k) &< M z_i^{\leq 0}(k), \\ P_i(k) &\leq M(1 - z_i^{\leq 0}(k)); \end{aligned} \tag{22b}$$

$$\begin{aligned} P_i(k) - P_i^{\text{STB}} &< M z_i^{\geq P_i^{\text{STB}}}(k), \\ -P_i(k) + P_i^{\text{STB}} &\leq M(1 - z_i^{\geq P_i^{\text{STB}}}(k)); \end{aligned} \tag{22c}$$

$$-P_i(k) + P_i^{\text{STB}} < M z_i^{\leq P_i^{\text{STB}}}(k), \quad P_i(k) - P_i^{\text{STB}} \leq M(1 - z_i^{\leq P_i^{\text{STB}}}(k)); \tag{22d}$$

$$P_i(k) - P_i^{\min} < M z_i^{\geq P_i^{\min}}(k), \quad -P_i(k) + P_i^{\min} \leq M(1 - z_i^{\geq P_i^{\min}}(k)); \tag{22e}$$

$$-P_i(k) + P_i^{\max} < M z_i^{\leq P_i^{\max}}(k), \quad P_i(k) - P_i^{\max} \leq M(1 - z_i^{\leq P_i^{\max}}(k)), \tag{22f}$$

that is, the logical variables $\delta_i^{\alpha}(k)$ can be now determined in terms of $z_i^{\geq \gamma}(k), z_i^{\leq \bar{\gamma}}(k)$, by means of

$$(1 - \delta_i^{\text{ON}}(k)) + z_i^{\geq P_i^{\min}}(k) \geq 1, \tag{23a}$$

$$(1 - \delta_i^{\text{ON}}(k)) + z_i^{\leq P_i^{\max}}(k) \geq 1; \tag{23b}$$

$$(1 - \delta_i^{\text{STB}}(k)) + z_i^{\geq P_i^{\text{STB}}}(k) \geq 1, \tag{23c}$$

$$(1 - \delta_i^{\text{STB}}(k)) + z_i^{\leq P_i^{\text{STB}}}(k) \geq 1; \tag{23d}$$

$$(1 - \delta_i^{\text{OFF}}(k)) + z_i^{\geq 0}(k) \geq 1, \tag{23e}$$

$$(1 - \delta_i^{\text{OFF}}(k)) + z_i^{\leq 0}(k) \geq 1; \tag{23f}$$

$$\delta_i^{\text{ON}}(k) + \delta_i^{\text{OFF}}(k) + \delta_i^{\text{STB}}(k) = 1. \tag{23g}$$

Notice that, despite $\delta_i^{\alpha}(k)$ being continuous, they can only assume the binary values $\{0, 1\}$ due to (23), that is in practice $\delta_i^{\alpha}(k)$s are logical.

A.2 Intraday Market Mathematical Model and Constraints Formulation of the State Transitions

As discussed above, the devices' models are characterized by three discrete operational states. These operational states imply possible mode transitions for each device. In what follows, we define all of the transitions. The transitions among the states for each transition is the result of the state change and can be defined by suitably combining logical variables, thus achieving

$$\sigma_{\text{ON}_i}^{\text{OFF}}(k) = \delta_i^{\text{ON}}(k-1) \wedge \delta_i^{\text{OFF}}(k), \tag{24a}$$

$$\sigma_{\text{OFF}_i}^{\text{ON}}(k) = \delta_i^{\text{OFF}}(k-1) \wedge \delta_i^{\text{ON}}(k), \tag{24b}$$

$$\sigma_{\text{ON}_i}^{\text{STB}}(k) = \delta_i^{\text{ON}}(k-1) \wedge \delta_i^{\text{STB}}(k), \tag{24c}$$

$$\sigma_{\text{STB}_i}^{\text{ON}}(k) = \delta_i^{\text{STB}}(k-1) \wedge \delta_i^{\text{ON}}(k), \tag{24d}$$

$$\sigma_{\text{STB}_i}^{\text{OFF}}(k) = \delta_i^{\text{STB}}(k-1) \wedge \delta_i^{\text{OFF}}(k), \tag{24e}$$

$$\sigma_{\text{OFF}_i}^{\text{STB}}(k) = \delta_i^{\text{OFF}}(k-1) \wedge \delta_i^{\text{STB}}(k), \tag{24f}$$

with $\alpha, \beta \in \{\text{OFF}, \text{STB}, \text{ON}\}$, $\alpha \neq \beta$. Using the relationships defined by Bemporad and Morari in [6], each expression of (24) is equivalently converted into three inequalities and introduced in the constraints of MPC controller, thus resulting in the 18 following formulas:

$$\begin{aligned} -\delta_i^{\text{ON}}(k-1) + \sigma_{\text{ON}_i}^{\text{OFF}}(k) &\leq 0, \\ -\delta_i^{\text{OFF}}(k) + \sigma_{\text{ON}_i}^{\text{OFF}}(k) &\leq 0, \\ \delta_i^{\text{ON}}(k-1) + \delta_i^{\text{OFF}}(k) - \sigma_{\text{ON}_i}^{\text{OFF}}(k) &\leq 1; \end{aligned} \tag{25a}$$

$$\begin{aligned} -\delta_i^{\text{OFF}}(k-1) + \sigma_{\text{OFF}_i}^{\text{ON}}(k) &\leq 0, \\ -\delta_i^{\text{ON}}(k) + \sigma_{\text{OFF}_i}^{\text{ON}}(k) &\leq 0, \\ \delta_i^{\text{OFF}}(k-1) + \delta_i^{\text{ON}}(k) - \sigma_{\text{OFF}_i}^{\text{ON}}(k) &\leq 1; \end{aligned} \tag{25b}$$

$$\begin{aligned} -\delta_i^{\text{ON}}(k-1) + \sigma_{\text{ON}_i}^{\text{STB}}(k) &\leq 0, \\ -\delta_i^{\text{STB}}(k) + \sigma_{\text{ON}_i}^{\text{STB}}(k) &\leq 0, \\ \delta_i^{\text{ON}}(k-1) + \delta_i^{\text{STB}}(k) - \sigma_{\text{ON}_i}^{\text{STB}}(k) &\leq 1; \end{aligned} \tag{25c}$$

$$\begin{aligned} -\delta_i^{\text{STB}}(k-1) + \sigma_{\text{STB}_i}^{\text{ON}}(k) &\leq 0, \\ -\delta_i^{\text{ON}}(k) + \sigma_{\text{STB}_i}^{\text{ON}}(k) &\leq 0, \\ \delta_i^{\text{STB}}(k-1) + \delta_i^{\text{ON}}(k) - \sigma_{\text{STB}_i}^{\text{ON}}(k) &\leq 1; \end{aligned} \tag{25d}$$

$$\begin{aligned} -\delta_i^{\text{STB}}(k-1) + \sigma_{\text{STB}_i}^{\text{OFF}}(k) &\leq 0, \\ -\delta_i^{\text{OFF}}(k) + \sigma_{\text{STB}_i}^{\text{OFF}}(k) &\leq 0, \\ \delta_i^{\text{STB}}(k-1) + \delta_i^{\text{OFF}}(k) - \sigma_{\text{STB}_i}^{\text{OFF}}(k) &\leq 1; \end{aligned} \tag{25e}$$

$$\begin{aligned} -\delta_i^{\text{OFF}}(k-1) + \sigma_{\text{OFF}_i}^{\text{STB}}(k) &\leq 0, \\ -\delta_i^{\text{STB}}(k) + \sigma_{\text{OFF}_i}^{\text{STB}}(k) &\leq 0, \\ \delta_i^{\text{OFF}}(k-1) + \delta_i^{\text{STB}}(k) - \sigma_{\text{OFF}_i}^{\text{STB}}(k) &\leq 1, \end{aligned} \tag{25f}$$

where $\sigma_{\alpha_i}^{\beta} \in [0, 1]$, and analogously to $\delta_i^{\alpha}(k)$s, they can only assume values $\{0, 1\}$ due to (25).

A.3 Intraday Market Controller Grid MLD Formulation

The conversions introduced in [6] make it possible to include binary and auxiliary variables introduced in a discrete-time dynamic system in order to describe, in a unified model, the evolution of the continuous and logic signals of the system. Thus,

$$\delta_{\text{sale}}^{\text{HL}}(k) = \begin{cases} 0, & P_{\text{sale}}^{\text{HL}}(k) = 0, \\ 1, & P_{\text{sale}}^{\text{HL}}(k) = P_{\text{grid}}(k) \end{cases} \tag{26}$$

where

$$P_{\text{sale}}^{\text{HL}}(k) = P_{\text{grid}}(k)\delta_{\text{sale}}^{\text{HL}}(k) \tag{27}$$

$$\begin{cases} P^{\text{HL}}_{\text{sale}}(k) & \leq M_{\text{sale}}\delta^{\text{HL}}_{\text{sale}}(k) \\ P^{\text{HL}}_{\text{sale}}(k) & \geq m_{\text{sale}}\delta^{\text{HL}}_{\text{sale}}(k) \\ P^{\text{HL}}_{\text{sale}}(k) & \leq P_{\text{grid}}(k) - m_{\text{sale}}(1-\delta^{\text{HL}}_{\text{sale}}(k)) \\ P^{\text{HL}}_{\text{sale}}(k) & \geq P_{\text{grid}}(k) - M_{\text{sale}}(1-\delta^{\text{HL}}_{\text{sale}}(k)). \end{cases} \tag{28a}$$

A.4 High-level MPC Controller

According to the MPC scheme, at each instant k, a sequence of future command inputs is selected by the controller using an optimization procedure that minimizes the cost functions and, at the same time, imposes the fulfillment of the constraints. The first sample of the control sequence is considered only, and subsequently, the horizon is shifted. Let us now introduce the set $\mathscr{C}$ of all the decision variable vectors defined as

$$\mathscr{C}_k := \left\{ \boldsymbol{P}^{T-1}_{\text{i},k}, \boldsymbol{P}^{T-1}_{\text{avl},k}, \mathbf{P}^{T-1}_{w,k}, \boldsymbol{\delta}^{\alpha,T-1}_{\text{i},k}, \boldsymbol{\sigma}^{\beta,T-1}_{\alpha,\text{i},k}, \boldsymbol{z}^{\geq\gamma,T-1}_{\text{i},k}, \boldsymbol{z}^{\leq\bar{\gamma},T-1}_{\text{i},k}, \boldsymbol{P}^{T-1}_{\text{grid},k} \right\} \tag{29}$$

where

$$\boldsymbol{P}^{T-1}_{\text{i},k} := \Big(P_{\text{i}}(k), \quad \dots \quad , P_{\text{i}}(k+T-1) \Big)^{\top}, \tag{30a}$$

$$\boldsymbol{P}^{T-1}_{w,k} := \Big(P_{w}(k), \quad \dots \quad , P_{w}(k+T-1) \Big)^{\top}, \tag{30b}$$

$$\boldsymbol{\delta}^{\alpha,T-1}_{\text{i},k} := \Big(\delta^{\alpha}_{\text{i}}(k), \quad \dots \quad , \delta^{\alpha}_{\text{i}}(k+T-1) \Big)^{\top}, \tag{30c}$$

$$\boldsymbol{\sigma}^{\beta,T-1}_{\alpha,\text{i},k} := \Big(\sigma^{\beta}_{\alpha,\text{i}}(k), \quad \dots \quad , \sigma^{\beta}_{\alpha,\text{i}}(k+T-1) \Big)^{\top}, \tag{30d}$$

$$\boldsymbol{z}^{\leq\bar{\gamma},T-1}_{\text{i},k} := \Big(z^{\leq\bar{\gamma}}_{\text{i}}(k), \quad \dots \quad , z^{\leq\bar{\gamma}}_{\text{i}}(k+T-1) \Big)^{\top}, \tag{30e}$$

$$\boldsymbol{z}^{\geq\gamma,T-1}_{\text{i},k} := \Big(z^{\geq\gamma}_{\text{i}}(k), \quad \dots \quad , z^{\geq\gamma}_{\text{i}}(k+T-1) \Big)^{\top}. \tag{30f}$$

In other words, the problem is recast as

$$\begin{aligned} \underset{\mathscr{C}_k}{\text{minimize}} \quad & \sum_{j=0}^{T-1} \rho_l J_l(k+j) + \rho_g J_g(k+j) + \rho_e J_e(k+j) + \rho_f J_f(k+j) \\ \text{subject to} \quad & (1), (5), (6), (22)-(23), (25), \\ & H \geq H^*, \\ & \delta^{\alpha}_i, \delta^{\beta}_{\alpha_i} \in [0,1] \qquad\qquad \alpha, \beta \in \{\text{OFF}, \text{ON}, \text{STB}\}, \alpha \neq \beta, \\ & z^{\geq\gamma}_i, z^{\leq\bar{\gamma}}_i \in \{0,1\} \qquad\qquad (\gamma, \bar{\gamma}) \in \{(0,0), (P^{\min}_i, P^{\max}_i), (P^{\text{STB}}_i, P^{\text{STB}}_i)\}. \end{aligned}$$

where

$$H^* = \underset{\mathscr{C}_k}{\arg\min} \quad \sum_{j=0}^{T-1} J_{\text{FCEV}}(k+j)$$

$$
\begin{aligned}
\text{subject to} \quad & (1), (5), (6), (22) - (23), (25), \\
& \delta_i^{\alpha}, \delta_{\alpha_i}^{\beta} \in [0,1] && \alpha, \beta \in \{\text{OFF}, \text{ON}, \text{STB}\}, \alpha \neq \beta, \\
& z_i^{\geq \gamma}, z_i^{\leq \bar{\gamma}} \in \{0,1\} && (\gamma, \bar{\gamma}) \in \{(0,0), (P_i^{\min}, P_i^{\max}), (P_i^{\text{STB}}, P_i^{\text{STB}})\}.
\end{aligned}
$$

where T is the simulation horizon and ρ_l, ρ_g, ρ_e and ρ_f are the wheights of the load tracking, grid participation, electrolyzer operating and fuel cell operating cost functions, respectively, that can be tuned so as to achieve a desired prioritization among them.

B Appendix B

B.1 Real-time Market Constraints Formulation of the Logical States

According to the operating condition of the electrolyzer and of the fuel cell, each $\delta_i^{\alpha}(k)$ with $i \in \{e, f\}$ is determined at any time-step k as follows

$$
\begin{cases}
P_i^{\min} \leq P_i(k) \leq P_i^{\max} & \iff \delta_i^{\text{ON}} = 1, \\
P_i(k) = P_i^{\text{CLD}} & \iff \delta_i^{\text{CLD}} = 1, \\
P_i(k) = P_i^{\text{STB}} & \iff \delta_i^{\text{STB}} = 1, \\
P_i(k) = P_i^{\text{WRM}} & \iff \delta_i^{\text{WRM}} = 1, \\
P_i(k) = 0 & \iff \delta_i^{\text{OFF}} = 1.
\end{cases} \tag{31}
$$

In order to derive mixed-integer constraints from (31), we introduce 20 auxiliary Boolean variables $z_i^{\gamma}(k) \in \{0,1\}$ with $i \in \{e, f\}$ and $\gamma \in \{\geq 0, \leq 0, \geq P_i^{\text{CLD}}, \leq P_i^{\text{CLD}}, \geq P_i^{\text{STB}}, \leq P_i^{\text{STB}}, \geq P_i^{\text{WRM}}, \leq P_i^{\text{WRM}}, \geq P_i^{\min}, \leq P_i^{\max}\}$, defined as

$$
z_i^{\geq 0}(k) = \begin{cases} 1 & P_i(k) \geq 0, \\ 0 & P_i(k) < 0, \end{cases} \tag{32a}
$$

$$
z_i^{\leq 0}(k) = \begin{cases} 0 & P_i(k) > 0, \\ 1 & P_i(k) \leq 0, \end{cases} \tag{32b}
$$

$$
z_i^{\geq P_i^{\text{CLD}}}(k) = \begin{cases} 1 & P_i(k) \geq P_i^{\text{CLD}}, \\ 0 & P_i(k) < P_i^{\text{CLD}}, \end{cases} \tag{32c}
$$

$$
z_i^{\leq P_i^{\text{CLD}}}(k) = \begin{cases} 0 & P_i(k) > P_i^{\text{CLD}}, \\ 1 & P_i(k) \leq P_i^{\text{CLD}}, \end{cases} \tag{32d}
$$

$$
z_i^{\geq P_i^{\text{STB}}}(k) = \begin{cases} 1 & P_i(k) \geq P_i^{\text{STB}}, \\ 0 & P_i(k) < P_i^{\text{STB}}, \end{cases} \tag{32e}
$$

$$
z_i^{\leq P_i^{\text{STB}}}(k) = \begin{cases} 0 & P_i(k) > P_i^{\text{STB}}, \\ 1 & P_i(k) \leq P_i^{\text{STB}}, \end{cases} \tag{32f}
$$

$$
z_i^{\geq P_i^{\text{WRM}}}(k) = \begin{cases} 1 & P_i(k) \geq P_i^{\text{WRM}}, \\ 0 & P_i(k) < P_i^{\text{WRM}}, \end{cases} \tag{32g}
$$

$$z_i^{\leq P_i^{\mathrm{WRM}}}(k) = \begin{cases} 0 & P_i(k) > P_i^{\mathrm{WRM}}, \\ 1 & P_i(k) \leq P_i^{\mathrm{WRM}}, \end{cases} \tag{32h}$$

$$z_i^{\geq P_i^{\min}}(k) = \begin{cases} 1 & P_i(k) \geq P_i^{\min}, \\ 0 & P_i(k) < P_i^{\min}, \end{cases} \tag{32i}$$

$$z_i^{\leq P_i^{\max}}(k) = \begin{cases} 0 & P_i(k) > P_i^{\max}, \\ 1 & P_i(k) \leq P_i^{\max}. \end{cases} \tag{32j}$$

Then, according to what in [6], (32) can be recasted as

$$\begin{aligned} P_i(k) &< M z_i^{\geq 0}(k), \\ -P_i(k) &\leq M(1 - z_i^{\geq 0}(k)); \end{aligned} \tag{33a}$$

$$\begin{aligned} -P_i(k) &< M z_i^{\leq 0}(k), \\ P_i(k) &\leq M(1 - z_i^{\leq 0}(k)); \end{aligned} \tag{33b}$$

$$\begin{aligned} P_i(k) - P_i^{\mathrm{CLD}} &< M z_i^{\geq P_i^{\mathrm{CLD}}}(k), \\ -P_i(k) + P_i^{\mathrm{CLD}} &\leq M(1 - z_i^{\geq P_i^{\mathrm{CLD}}}(k)); \end{aligned} \tag{33c}$$

$$\begin{aligned} -P_i(k) + P_i^{\mathrm{CLD}} &< M z_i^{\leq P_i^{\mathrm{CLD}}}(k), \\ P_i(k) - P_i^{\mathrm{CLD}} &\leq M(1 - z_i^{\leq P_i^{\mathrm{CLD}}}(k)); \end{aligned} \tag{33d}$$

$$\begin{aligned} P_i(k) - P_i^{\mathrm{STB}} &< M z_i^{\geq P_i^{\mathrm{STB}}}(k), \\ -P_i(k) + P_i^{\mathrm{STB}} &\leq M(1 - z_i^{\geq P_i^{\mathrm{STB}}}(k)); \end{aligned} \tag{33e}$$

$$\begin{aligned} -P_i(k) + P_i^{\mathrm{STB}} &< M z_i^{\leq P_i^{\mathrm{STB}}}(k), \\ P_i(k) - P_i^{\mathrm{STB}} &\leq M(1 - z_i^{\leq P_i^{\mathrm{STB}}}(k)); \end{aligned} \tag{33f}$$

$$\begin{aligned} P_i(k) - P_i^{\mathrm{WRM}} &< M z_i^{\geq P_i^{\mathrm{STB}}}(k), \\ -P_i(k) + P_i^{\mathrm{WRM}} &\leq M(1 - z_i^{\geq P_i^{\mathrm{STB}}}(k)); \end{aligned} \tag{33g}$$

$$\begin{aligned} -P_i(k) + P_i^{\mathrm{WRM}} &< M z_i^{\leq P_i^{\mathrm{WRM}}}(k), \\ P_i(k) - P_i^{\mathrm{WRM}} &\leq M(1 - z_i^{\leq P_i^{\mathrm{WRM}}}(k)); \end{aligned} \tag{33h}$$

$$\begin{aligned} P_i(k) - P_i^{\min} &< M z_i^{\geq P_i^{\min}}(k), \\ -P_i(k) + P_i^{\min} &\leq M(1 - z_i^{\geq P_i^{\min}}(k)); \end{aligned} \tag{33i}$$

$$\begin{aligned} -P_i(k) + P_i^{\max} &< M z_i^{\leq P_i^{\max}}(k), \\ P_i(k) - P_i^{\max} &\leq M(1 - z_i^{\leq P_i^{\max}}(k)). \end{aligned} \tag{33j}$$

That is, the logical variables $\delta_i^{\alpha}(k)$ can be now determined in terms of $z_i^{\geq \gamma}(k), z_i^{\leq \bar{\gamma}}(k)$, by means of

$$(1-\delta_i^{\mathrm{ON}}(k))+z_i^{\geq P_i^{\min}}(k)\geq 1, \tag{34a}$$
$$(1-\delta_i^{\mathrm{ON}}(k))+z_i^{\leq P_i^{\max}}(k)\geq 1; \tag{34b}$$
$$(1-\delta_i^{\mathrm{CLD}}(k))+z_i^{\geq P_i^{\mathrm{CLD}}}(k)\geq 1, \tag{34c}$$
$$(1-\delta_i^{\mathrm{CLD}}(k))+z_i^{\leq P_i^{\mathrm{CLD}}}(k)\geq 1; \tag{34d}$$
$$(1-\delta_i^{\mathrm{STB}}(k))+z_i^{\geq P_i^{\mathrm{STB}}}(k)\geq 1, \tag{34e}$$
$$(1-\delta_i^{\mathrm{STB}}(k))+z_i^{\leq P_i^{\mathrm{STB}}}(k)\geq 1; \tag{34f}$$
$$(1-\delta_i^{\mathrm{WRM}}(k))+z_i^{\geq P_i^{\mathrm{WRM}}}(k)\geq 1, \tag{34g}$$
$$(1-\delta_i^{\mathrm{WRM}}(k))+z_i^{\leq P_i^{\mathrm{WRM}}}(k)\geq 1; \tag{34h}$$
$$(1-\delta_i^{\mathrm{OFF}}(k))+z_i^{\geq 0}(k)\geq 1, \tag{34i}$$
$$(1-\delta_i^{\mathrm{OFF}}(k))+z_i^{\leq 0}(k)\geq 1; \tag{34j}$$
$$\delta_i^{\mathrm{ON}}(k)+\delta_i^{\mathrm{OFF}}(k)+\delta_i^{\mathrm{STB}}(k)+\delta_i^{\mathrm{CLD}}(k)+\delta_i^{\mathrm{WRM}}(k)=1. \tag{34k}$$

Notice that, despite $\delta_i^{\alpha}(k)$ being continuous, they can only assume the binary values $\{0,1\}$ due to (34), that us in practice $\delta_i^{\alpha}(k)s$ are logical.

B.2 Real-time Market Mathematical Model and Constraints Formulation of the State Transitions

States' transitions can be defined as

$$\sigma_{\mathrm{OFF}_i}^{\mathrm{ON}}(k)=\delta_i^{\mathrm{OFF}}(k-1)\wedge\delta_i^{\mathrm{ON}}(k), \tag{35a}$$
$$\sigma_{\mathrm{OFF}_i}^{\mathrm{WRM}}(k)=\delta_i^{\mathrm{OFF}}(k-1)\wedge\delta_i^{\mathrm{WRM}}(k), \tag{35b}$$
$$\sigma_{\mathrm{OFF}_i}^{\mathrm{STB}}(k)=\delta_i^{\mathrm{OFF}}(k-1)\wedge\delta_i^{\mathrm{STB}}(k), \tag{35c}$$
$$\sigma_{\mathrm{CLD}_i}^{\mathrm{OFF}}(k)=\delta_i^{\mathrm{CLD}}(k-1)\wedge\delta_i^{\mathrm{OFF}}(k), \tag{35d}$$
$$\sigma_{\mathrm{CLD}_i}^{\mathrm{ON}}(k)=\delta_i^{\mathrm{CLD}}(k-1)\wedge\delta_i^{\mathrm{ON}}(k), \tag{35e}$$
$$\sigma_{\mathrm{CLD}_i}^{\mathrm{WRM}}(k)=\delta_i^{\mathrm{CLD}}(k-1)\wedge\delta_i^{\mathrm{WRM}}(k), \tag{35f}$$
$$\sigma_{\mathrm{STB}_i}^{\mathrm{ON}}(k)=\delta_i^{\mathrm{STB}}(k-1)\wedge\delta_i^{\mathrm{ON}}(k), \tag{35g}$$
$$\sigma_{\mathrm{STB}_i}^{\mathrm{CLD}}(k)=\delta_i^{\mathrm{STB}}(k-1)\wedge\delta_i^{\mathrm{CLD}}(k), \tag{35h}$$
$$\sigma_{\mathrm{WRM}_i}^{\mathrm{OFF}}(k)=\delta_i^{\mathrm{WRM}}(k-1)\wedge\delta_i^{\mathrm{OFF}}(k), \tag{35i}$$
$$\sigma_{\mathrm{WRM}_i}^{\mathrm{CLD}}(k)=\delta_i^{\mathrm{WRM}}(k-1)\wedge\delta_i^{\mathrm{CLD}}(k), \tag{35j}$$
$$\sigma_{\mathrm{WRM}_i}^{\mathrm{STB}}(k)=\delta_i^{\mathrm{WRM}}(k-1)\wedge\delta_i^{\mathrm{STB}}(k), \tag{35k}$$

$$\sigma_{\mathrm{ON}_i}^{\mathrm{CLD}}(k) = \delta_i^{\mathrm{ON}}(k-1) \wedge \delta_i^{\mathrm{CLD}}(k), \tag{35l}$$

$$\sigma_{\mathrm{ON}_i}^{\mathrm{WRM}}(k) = \delta_i^{\mathrm{ON}}(k-1) \wedge \delta_i^{\mathrm{WRM}}(k), \tag{35m}$$

$$\sigma_{\mathrm{CLD}_i}^{\mathrm{STB}}(k) = \delta_i^{\mathrm{CLD}}(k-1) \wedge \delta_i^{\mathrm{STB}}(k), \tag{35n}$$

$$\sigma_{\mathrm{STB}_i}^{\mathrm{OFF}}(k) = \delta_i^{\mathrm{STB}}(k-1) \wedge \delta_i^{\mathrm{OFF}}(k), \tag{35o}$$

$$\sigma_{\mathrm{ON}_i}^{\mathrm{OFF}}(k) = \delta_i^{\mathrm{ON}}(k-1) \wedge \delta_i^{\mathrm{OFF}}(k). \tag{35p}$$

Based on the formulation in [6], the expressions above can be converted into the inequalities:

$$\begin{aligned}
-\delta_i^{\mathrm{OFF}}(k-1) + \sigma_{\mathrm{OFF}_i}^{\mathrm{ON}}(k) &\leq 0,\\
-\delta_i^{\mathrm{ON}}(k) + \sigma_{\mathrm{OFF}_i}^{\mathrm{ON}}(k) &\leq 0,\\
\delta_i^{\mathrm{OFF}}(k-1) + \delta_i^{\mathrm{ON}}(k) - \sigma_{\mathrm{OFF}_i}^{\mathrm{ON}}(k) &\leq 1;
\end{aligned} \tag{36a}$$

$$\begin{aligned}
-\delta_i^{\mathrm{OFF}}(k-1) + \sigma_{\mathrm{OFF}_i}^{\mathrm{WRM}}(k) &\leq 0,\\
-\delta_i^{\mathrm{WRM}}(k) + \sigma_{\mathrm{OFF}_i}^{\mathrm{WRM}}(k) &\leq 0,\\
\delta_i^{\mathrm{OFF}}(k-1) + \delta_i^{\mathrm{WRM}}(k) - \sigma_{\mathrm{OFF}_i}^{\mathrm{WRM}}(k) &\leq 1;
\end{aligned} \tag{36b}$$

$$\begin{aligned}
-\delta_i^{\mathrm{OFF}}(k-1) + \sigma_{\mathrm{OFF}_i}^{\mathrm{STB}}(k) &\leq 0,\\
-\delta_i^{\mathrm{STB}}(k) + \sigma_{\mathrm{OFF}_i}^{\mathrm{STB}}(k) &\leq 0,\\
\delta_i^{\mathrm{OFF}}(k-1) + \delta_i^{\mathrm{STB}}(k) - \sigma_{\mathrm{OFF}_i}^{\mathrm{STB}}(k) &\leq 1;
\end{aligned} \tag{36c}$$

$$\begin{aligned}
-\delta_i^{\mathrm{CLD}}(k-1) + \sigma_{\mathrm{CLD}_i}^{\mathrm{OFF}}(k) &\leq 0,\\
-\delta_i^{\mathrm{OFF}}(k) + \sigma_{\mathrm{CLD}_i}^{\mathrm{OFF}}(k) &\leq 0,\\
\delta_i^{\mathrm{CLD}}(k-1) + \delta_i^{\mathrm{OFF}}(k) - \sigma_{\mathrm{CLD}_i}^{\mathrm{OFF}}(k) &\leq 1;
\end{aligned} \tag{36d}$$

$$\begin{aligned}
-\delta_i^{\mathrm{CLD}}(k-1) + \sigma_{\mathrm{CLD}_i}^{\mathrm{ON}}(k) &\leq 0,\\
-\delta_i^{\mathrm{ON}}(k) + \sigma_{\mathrm{CLD}_i}^{\mathrm{ON}}(k) &\leq 0,\\
\delta_i^{\mathrm{CLD}}(k-1) + \delta_i^{\mathrm{WRM}}(k) - \sigma_{\mathrm{CLD}_i}^{\mathrm{ON}}(k) &\leq 1;
\end{aligned} \tag{36e}$$

$$\begin{aligned}
-\delta_i^{\mathrm{CLD}}(k-1) + \sigma_{\mathrm{CLD}_i}^{\mathrm{WRM}}(k) &\leq 0,\\
-\delta_i^{\mathrm{WRM}}(k) + \sigma_{\mathrm{CLD}_i}^{\mathrm{WRM}}(k) &\leq 0,\\
\delta_i^{\mathrm{CLD}}(k-1) + \delta_i^{\mathrm{WRM}}(k) - \sigma_{\mathrm{CLD}_i}^{\mathrm{WRM}}(k) &\leq 1;
\end{aligned} \tag{36f}$$

$$\begin{aligned}
-\delta_i^{\mathrm{STB}}(k-1) + \sigma_{\mathrm{STB}_i}^{\mathrm{ON}}(k) &\leq 0,\\
-\delta_i^{\mathrm{ON}}(k) + \sigma_{\mathrm{STB}_i}^{\mathrm{ON}}(k) &\leq 0,\\
\delta_i^{\mathrm{STB}}(k-1) + \delta_i^{\mathrm{WRM}}(k) - \sigma_{\mathrm{STB}_i}^{\mathrm{ON}}(k) &\leq 1;
\end{aligned} \tag{36g}$$

$$\begin{aligned}
-\delta_i^{\mathrm{STB}}(k-1) + \sigma_{\mathrm{STB}_i}^{\mathrm{CLD}}(k) &\leq 0,\\
-\delta_i^{\mathrm{CLD}}(k) + \sigma_{\mathrm{STB}_i}^{\mathrm{CLD}}(k) &\leq 0,\\
\delta_i^{\mathrm{STB}}(k-1) + \delta_i^{\mathrm{CLD}}(k) - \sigma_{\mathrm{STB}_i}^{\mathrm{CLD}}(k) &\leq 1;
\end{aligned} \tag{36h}$$

$$
\begin{aligned}
-\delta_i^{\mathrm{WRM}}(k-1)+\sigma_{\mathrm{WRM}_i}^{\mathrm{OFF}}(k) &\leq 0,\\
-\delta_i^{\mathrm{OFF}}(k)+\sigma_{\mathrm{WRM}_i}^{\mathrm{OFF}}(k) &\leq 0, \qquad (36i)\\
\delta_i^{\mathrm{WRM}}(k-1)+\delta_i^{\mathrm{OFF}}(k)-\sigma_{\mathrm{WRM}_i}^{\mathrm{OFF}}(k) &\leq 1;\\
-\delta_i^{\mathrm{WRM}}(k-1)+\sigma_{\mathrm{WRM}_i}^{\mathrm{CLD}}(k) &\leq 0,\\
-\delta_i^{\mathrm{CLD}}(k)+\sigma_{\mathrm{WRM}_i}^{\mathrm{CLD}}(k) &\leq 0, \qquad (36j)\\
\delta_i^{\mathrm{WRM}}(k-1)+\delta_i^{\mathrm{CLD}}(k)-\sigma_{\mathrm{WRM}_i}^{\mathrm{CLD}}(k) &\leq 1;\\
-\delta_i^{\mathrm{WRM}}(k-1)+\sigma_{\mathrm{WRM}_i}^{\mathrm{STB}}(k) &\leq 0,\\
-\delta_i^{\mathrm{STB}}(k)+\sigma_{\mathrm{WRM}_i}^{\mathrm{STB}}(k) &\leq 0, \qquad (36k)\\
\delta_i^{\mathrm{WRM}}(k-1)+\delta_i^{\mathrm{STB}}(k)-\sigma_{\mathrm{WRM}_i}^{\mathrm{STB}}(k) &\leq 1;\\
-\delta_i^{\mathrm{ON}}(k-1)+\sigma_{\mathrm{ON}_i}^{\mathrm{CLD}}(k) &\leq 0,\\
-\delta_i^{\mathrm{CLD}}(k)+\sigma_{\mathrm{ON}_i}^{\mathrm{CLD}}(k) &\leq 0, \qquad (36l)\\
\delta_i^{\mathrm{ON}}(k-1)+\delta_i^{\mathrm{CLD}}(k)-\sigma_{\mathrm{ON}_i}^{\mathrm{CLD}}(k) &\leq 1;\\
-\delta_i^{\mathrm{ON}}(k-1)+\sigma_{\mathrm{ON}_i}^{\mathrm{WRM}}(k) &\leq 0,\\
-\delta_i^{\mathrm{WRM}}(k)+\sigma_{\mathrm{ON}_i}^{\mathrm{WRM}}(k) &\leq 0, \qquad (36m)\\
\delta_i^{\mathrm{ON}}(k-1)+\delta_i^{\mathrm{WRM}}(k)-\sigma_{\mathrm{ON}_i}^{\mathrm{WRM}}(k) &\leq 1;\\
-\delta_i^{\mathrm{CLD}}(k-1)+\sigma_{\mathrm{CLD}_i}^{\mathrm{STB}}(k) &\leq 0,\\
-\delta_i^{\mathrm{STB}}(k)+\sigma_{\mathrm{CLD}_i}^{\mathrm{STB}}(k) &\leq 0, \qquad (36n)\\
\delta_i^{\mathrm{CLD}}(k-1)+\delta_i^{\mathrm{STB}}(k)-\sigma_{\mathrm{CLD}_i}^{\mathrm{STB}}(k) &\leq 1;\\
-\delta_i^{\mathrm{STB}}(k-1)+\sigma_{\mathrm{STB}_i}^{\mathrm{OFF}}(k) &\leq 0,\\
-\delta_i^{\mathrm{OFF}}(k)+\sigma_{\mathrm{STB}_i}^{\mathrm{OFF}}(k) &\leq 0, \qquad (36o)\\
\delta_i^{\mathrm{STB}}(k-1)+\delta_i^{\mathrm{OFF}}(k)-\sigma_{\mathrm{STB}_i}^{\mathrm{OFF}}(k) &\leq 1;\\
-\delta_i^{\mathrm{ON}}(k-1)+\sigma_{\mathrm{ON}_i}^{\mathrm{OFF}}(k) &\leq 0,\\
-\delta_i^{\mathrm{OFF}}(k)+\sigma_{\mathrm{ON}_i}^{\mathrm{OFF}}(k) &\leq 0, \qquad (36p)\\
\delta_i^{\mathrm{ON}}(k-1)+\delta_i^{\mathrm{OFF}}(k)-\sigma_{\mathrm{ON}_i}^{\mathrm{OFF}}(k) &\leq 1.
\end{aligned}
$$

As discussed above in the modeling section, our system is constrained to evolve only the admissible transitions, namely the ones depicted in Figure 4. For some of them, i.e., $\sigma_{\mathrm{ON}_i}^{\mathrm{OFF}}(k)$, $\sigma_{\mathrm{CLD}_i}^{\mathrm{STB}}(k)$, and $\sigma_{\mathrm{STD}_i}^{\mathrm{OFF}}(k)$ a cost is paid due to the stack degradation in switching from hydrogen production (or consumption) and not production (or consumption) and vice versa. These transitions have been explicitly modeled since they will appear in the devices' cost functions. Furthermore, all the inadmissible transitions, i.e., all the ones other than those in Figure 4, have been defined and set to zero. It is important to highlight that, in order to force the evolution of the electrolyzer and the fuel cell modes according to each corresponding automaton as depicted in Figure 4, for $i \in \{e, f\}$, in (36) all the transitions of the not appearing edges are set to zero, that

is

$$\sigma^{\text{STB}}_{\text{OFF}_i}(k) = \sigma^{\text{WRM}}_{\text{OFF}_i}(k) = \sigma^{\text{ON}}_{\text{OFF}_i}(k) = 0, \tag{37a}$$
$$\sigma^{\text{OFF}}_{\text{CLD}_i}(k) = \sigma^{\text{WRM}}_{\text{CLD}_i}(k) = \sigma^{\text{ON}}_{\text{CLD}_i}(k) = 0, \tag{37b}$$
$$\sigma^{\text{ON}}_{\text{STB}_i}(k) = \sigma^{\text{CLD}}_{\text{STB}_i}(k) = 0, \tag{37c}$$
$$\sigma^{\text{OFF}}_{\text{WRM}_i}(k) = \sigma^{\text{CLD}}_{\text{WRM}_i}(k) = \sigma^{\text{STB}}_{\text{WRM}_i}(k) = 0, \tag{37d}$$
$$\sigma^{\text{CLD}}_{\text{ON}_i}(k) = \sigma^{\text{WRM}}_{\text{ON}_i}(k) = 0. \tag{37e}$$

B.3 Hydrogen Level Dynamics

The hydrogen level dynamics are similar to those considered in the other use cases except that in the fuel-production use case we introduce a loss term $H^{\text{FCEV}}\delta_{\text{FCEV}}$ which models the use of the stored hydrogen for supplying demand from fuel cell electric vehicles:

$$H(k+1) = H(k) - H^{\text{FCEV}}\delta_{FCEV}(k) + \eta_e P_e(k)\delta^{\text{ON}}_e(k)T_s - \frac{P_f(k)\delta^{\text{ON}}_f(k)T_s}{\eta_f}. \tag{38}$$

where $Ts = 1$ min.

B.4 Power Balance Constraints

The power balance between energy production and consumption must be reached at each time-step k; hence the following equality constraint holds

$$P_w(k) - P_e(k)\delta^{\text{ON}}_e(k) + P_f(k)\delta^{\text{ON}}_f(k) - P_{\text{avl}}(k) = P_{\text{grid}}. \tag{39}$$

B.5 Real-time Market Controller Grid MLD Formulation

Starting from the definition of the logical variable $\delta_{\text{grid}}(k)$ in (2), the auxiliary variables $P^{\text{LL}}_{\text{sale}}(k)$ can be defined as

$$\delta^{\text{LL}}_{\text{sale}}(k,m) = \begin{cases} 1, & (P_{\text{grid}}(k,m) - P^{\text{sch}}_{\text{grid}}(k)) \geq 0 \\ 0, & (P_{\text{grid}}(k,m) - P^{\text{sch}}_{\text{grid}}(k)) < 0. \end{cases} \tag{40}$$

The variables $P^{\text{LL}}_{\text{sale}}(k)$ hide a non-linearity and model the selling events to the utility grid. The mixed-integer product of (40) cannot be directly handled by numerical solvers and, therefore, a further manipulation is needed. The variables defined above in (40) can be expressed as mixed-logic inequalities. Then, the selling microgrid behavior can be recast as

$$\begin{cases} P^{\text{LL}}_{\text{sale}}(k,m) & \leq M^{\text{LL}}_{\text{sale}}\delta^{\text{LL}}_{\text{sale}}(k,m), \\ P^{\text{LL}}_{\text{sale}}(k,m) & \geq m^{\text{LL}}_{\text{sale}}\delta^{\text{LL}}_{\text{sale}}(k,m), \\ P^{\text{LL}}_{\text{sale}}(k,m) & \leq P_{\text{grid}}(k,m) - m^{\text{LL}}_{\text{sale}}(1 - \delta^{\text{LL}}_{\text{sale}}(k,m)), \\ P^{\text{LL}}_{\text{sale}}(k,m) & \geq P_{\text{grid}}(k,m) - M^{\text{LL}}_{\text{sale}}(1 - \delta^{\text{LL}}_{\text{sale}}(k,m)). \end{cases} \tag{41}$$

B.6 Low-level MPC Controller

The state of the system $H(k)$ to be controlled evolves according to (1) and the corresponding state variable is denoted by $H(k+j)$, with $j > 0$ at time $k+j$. Let us now introduce the set $\mathscr{C}_{k,m}$ of all the decision variable vectors at instant k defined as

$$\mathscr{C}_{k,m} := \left\{ \boldsymbol{P}_{\mathrm{i},k}^{T-1}, \boldsymbol{P}_{\mathrm{avl},k,m}^{T-1}, \boldsymbol{\delta}_{\mathrm{i},k,m}^{\alpha,T-1}, \boldsymbol{\sigma}_{\alpha,\mathrm{i},k,m}^{\beta,T-1}, \boldsymbol{z}_{i,k,m}^{\geq\gamma,T-1}, \boldsymbol{z}_{i,k,m}^{\leq\bar{\gamma},T-1}, \boldsymbol{P}_{\mathrm{grid},k,m}^{T-1} \right\}, \tag{42}$$

where

$$\boldsymbol{P}_{\mathrm{i},k}^{T-1} := \left(P_{\mathrm{i}}(k), \quad \dots \quad , P_{\mathrm{i}}(k+T-1) \right)^{\top}, \tag{43a}$$

$$\boldsymbol{P}_{w,k}^{T-1} := \left(P_{w}(k), \quad \dots \quad , P_{w}(k+T-1) \right)^{\top}, \tag{43b}$$

$$\boldsymbol{\delta}_{\mathrm{i},k}^{\alpha,T-1} := \left(\delta_{\mathrm{i}}^{\alpha}(k), \quad \dots \quad , \delta_{\mathrm{i}}^{\alpha}(k+T-1) \right)^{\top}, \tag{43c}$$

$$\boldsymbol{\sigma}_{\alpha,\mathrm{i},k}^{\beta,T-1} := \left(\sigma_{\alpha,\mathrm{i}}^{\beta}(k), \quad \dots \quad , \sigma_{\alpha,\mathrm{i}}^{\beta}(k+T-1) \right)^{\top}, \tag{43d}$$

$$\boldsymbol{z}_{i,k}^{\leq\bar{\gamma},T-1} := \left(z_{\mathrm{i}}^{\leq\bar{\gamma}}(k), \quad \dots \quad , z_{\mathrm{i}}^{\leq\bar{\gamma}}(k+T-1) \right)^{\top}, \tag{43e}$$

$$\boldsymbol{z}_{i,k}^{\geq\gamma,T-1} := \left(z_{\mathrm{i}}^{\geq\gamma}(k), \quad \dots \quad , z_{\mathrm{i}}^{\geq\gamma}(k+T-1) \right)^{\top}, \tag{43f}$$

with $i \in I$, $\alpha, \beta \in A^{\mathrm{LL}}$ and $(\gamma, \bar{\gamma}) \in P^{\mathrm{LL}}$. For any given pair (k, m), the MPC problem for the low-level control is

$$\begin{aligned}
\underset{\mathscr{C}_{k,m}}{\text{minimize}} \quad & J^{\mathrm{LL}}(k,m) \\
\text{subject to} \quad & (33)-(34), (36)-(39), (41), \\
& \delta_i^{\alpha} \in [0,1], \\
& \sigma_{\alpha_i}^{\beta} \in [0,1], \\
& \alpha, \beta \in A^{\mathrm{LL}}, \alpha \neq \beta, \\
& z_i^{\geq\gamma} \in \{0,1\}, \\
& z_i^{\leq\bar{\gamma}} \in \{0,1\}, \\
& (\gamma, \bar{\gamma}) \in P^{\mathrm{LL}}, \\
& \delta^{\mathrm{grid}} \in \{0,1\}, \\
& i \in I.
\end{aligned} \tag{44}$$

Since for any given k the problem (44) is solved again at time instants $m+1, \dots, m+p-1$, an optimal feedback strategy is generated and applied at real-time.